nature cell biology

Axin determines cell fate by controlling the p53 activation threshold after DNA damage

Qinxi Li[1,2], Shuyong Lin[1,2], Xuan Wang[1,2], Guili Lian[1], Zailian Lu[1], Huiling Guo[1], Ka Ruan[1], Yanhai Wang[1], Zhiyun Ye[1], Jiahuai Han[1] and Sheng-Cai Lin[1,3]

Cells can undergo either cell-cycle arrest or apoptosis after genotoxic stress, based on p53 activity[1–6]. Here we show that cellular fate commitment depends on Axin forming distinct complexes with Pirh2, Tip60, HIPK2 and p53. In cells treated with sublethal doses of ultra-violet (UV) radiation or doxorubicin (Dox), Pirh2 abrogates Axin-induced p53 phosphorylation at Ser 46 catalysed by HIPK2, by competing with HIPK2 for binding to Axin. However, on lethal treatment, Tip60 interacts with Axin and abrogates Pirh2–Axin binding, forming an Axin–Tip60–HIPK2–p53 complex that allows maximal p53 activation to trigger apoptosis. We also provide evidence that the ATM/ATR pathway mediates the Axin–Tip60 complex assembly. An axin mutation promotes carcinogenesis in *Axin^{Fu}/+* (*Axin-Fused*) mice, consistent with a dominant-negative role for Axin^{Fu} in p53 activation. Thus, Axin is a critical determinant in p53-dependent tumour suppression in which Pirh2 and Tip60 have different roles in triggering cell-cycle arrest or apoptosis depending on the severity of genotoxic stress.

Cells can limit the effects of genotoxin-induced DNA damage either by initiating apoptosis or by undergoing cell-cycle arrest to activate DNA repair. The molecular mechanisms underlying this fate decision remain obscure. The outstanding question has thus concerned the manner in which p53 activity is controlled such that cells regulate their reactions according to the severity of damage. A recent major advance in our understanding of the regulation of p53 functions has come from studies on HIPK2 (homeodomain-interacting protein kinase 2), which interacts with, and phosphorylates, p53 at Ser 46. This phosphorylation has been shown to be a critical determinant for cellular commitment to either cell-cycle arrest or apoptosis in response to different doses of genotoxic stress, including UV and Dox[7–11]. Interestingly, on treatment with Dox at a sublethal dose that causes cell-cycle arrest but not apoptosis, HIPK2 is degraded through ubiquitylation by MDM2 (ref. 9).

Axin was initially identified as a negative regulator of Wnt signalling and its mutation leads to duplication of the axis[12,13]. It has emerged as a major scaffold for many other signalling pathways, including mTOR[14], JNK MAPK[15], parathyroid hormone[16] as well as for p53 signalling[17,18]. We have shown previously that Axin interacts with p53 in two ways, directly through the p53 middle (MID) domain and indirectly through HIPK2 at the p53 carboxyl terminus[17]. Axin functions in UV-induced cell death by activating p53 by phosphorylating it at Ser 46, which is catalysed by HIPK2 (ref. 18), suggesting that Axin might exert a physiological role in genotoxic responses. The *Axin^{Fu}* allele is generated by insertion of an intracisternal A-particle (IAP) at intron 6 (ref. 13); the large insertion blocks splicing of wild-type Axin. Thus, two Axin protein species are generated from the *Axin^{Fu}* allele, a C-terminal truncated protein designated Axin^{Fu-NT} (amino-acids 1–596) and wild-type Axin[19]. To investigate the longstanding question of why genetically transmitted inbred 129P4/RrRk *Fused* mice do not show a higher incidence of tumours, we treated the mice with the DNA-damaging reagent DMBA (7,12-dimethylbenz-a-anthracene), as described previously[20]. At 12 weeks post-treatment, a drastic increase in the number of tumours in the skin of the *Axin^{Fu}*/+ heterozygous mice was observed compared with wild-type mice ($P < 0.001$; Fig. 1a, b). The tumours showed characteristic papilloma morphology (Supplementary Information, Fig. S1a). To explore the functional association between the *Axin^{Fu}* mutation and the p53 system, we tested p53 transcriptional activity using a luciferase reporter in the mouse skin fibroblasts of both +/+ and *Axin^{Fu}*/+ mice, and observed a significant reduction in p53 transactivational activity in *Axin^{Fu}*/+ fibroblasts on lethal Dox treatment, compared with that in +/+ cells, suggesting that the mutant cells are defective in p53 signalling (Fig. 1c). In addition, we found that Axin^{Fu-NT} exerts a dominant-negative effect on Axin-induced p53 phosphorylation at Ser 46 (Fig. 1d), p53 transactivation activity (Supplementary Information, Fig. S1b) and on the induction of apoptosis (Fig. 1e), in H1299 cells. Mechanistically, Axin^{Fu-NT} retains the ability to bind to p53, but lacks a HIPK2-binding domain (located in the C terminus of wild-type Axin), therefore it lacks the ability to phosphorylate p53 (Fig. 1d; Supplementary Information, Fig. S1c). Consistently, Axin$^{Fu-NT\Delta MID}$, a mutant that lacks

[1]Key Laboratory for Cell Biology and Tumor Cell Engineering of the Ministry of Education, School of Life Sciences, Xiamen University, Fujian 361005, China.
[2]These authors contributed equally to this work.
[3]Correspondence should be addressed to S.C.L. (e-mail: linsc@xmu.edu.cn).

Received 16 March 2009; accepted May 2009; published online 23 August 2009; corrected online 28 August 2009; DOI: 10.1038/ncb1927

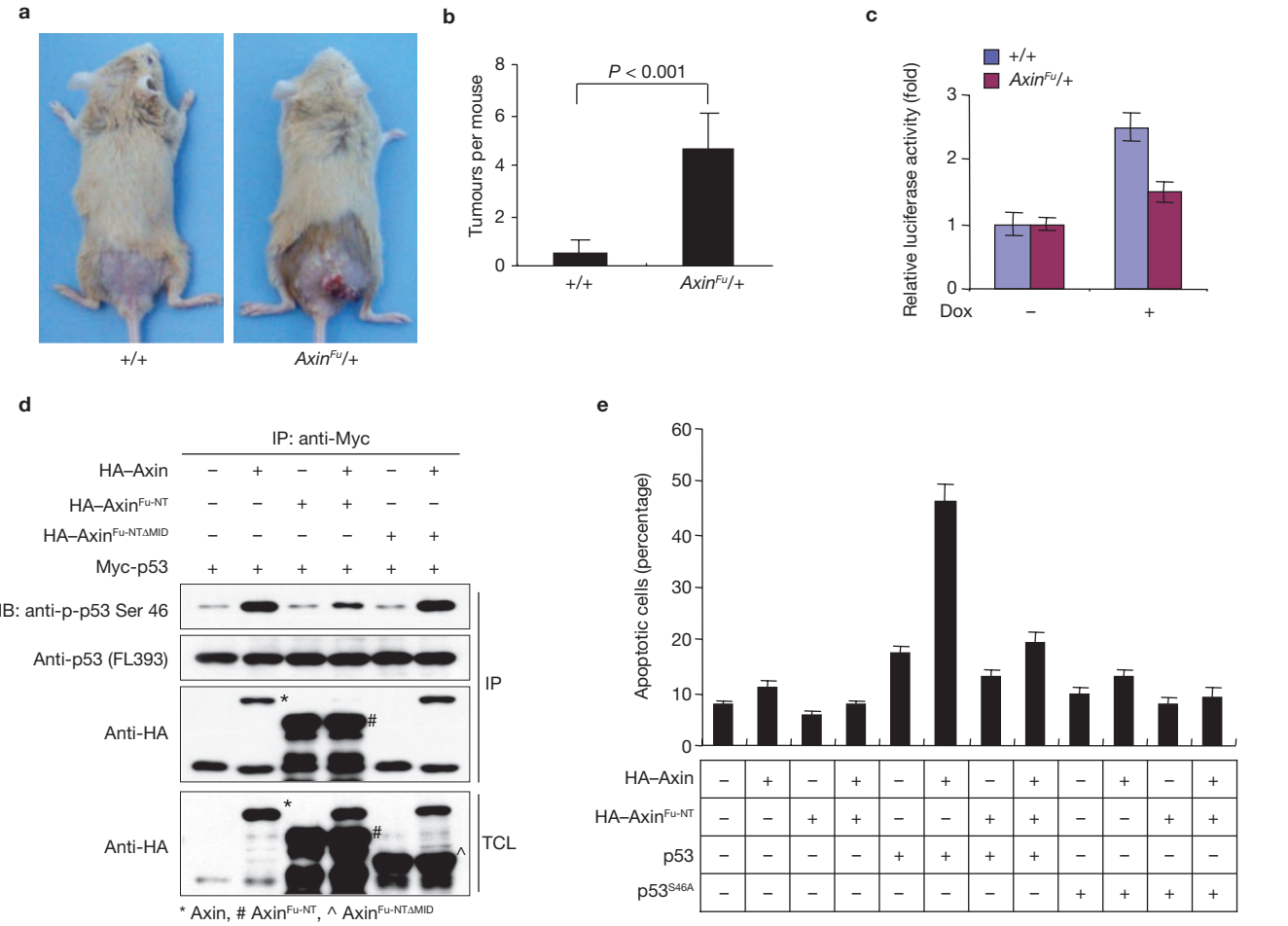

Figure 1 Mutation of *Axin* in *Axin*^{Fu}/+ mice promotes tumour formation. (**a**) Papillomas in wild-type and *Axin*^{Fu}/+ mice after 12 weeks of DMBA treatment. New born mice were treated with DMBA followed by TPA (12-O-tetra-decanoylphorbol-13-acetate) treatment twice a week. (**b**) The tumour numbers of DMBA-treated wild-type and *Axin*^{Fu}/+ mice were counted and subjected to statistical analysis using Student's *t*-test. Data are mean ± s.e.m. from three independent experiments in duplicate. (**c**) Reduced p53 transactivation activity in *Axin*^{Fu}/+ mouse skin fibroblasts. Primary *Axin*^{Fu}/+ and +/+ mouse skin fibroblasts were generated and transfected with a p53 luciferase reporter. At 24 h post-transfection, cells were left untreated or treated for 12 h with 2.5 μM Dox, before luciferase activity was measured. The results were normalized to LacZ activity and are mean ± s.e.m. from three separate experiments. (**d**) Axin^{Fu-NT} negatively regulates p53 Ser 46 phosphorylation induced by wild-type Axin. H1299 cells were transfected with Axin, Axin^{Fu-NT}, Axin$^{Fu-NT\Delta MID}$ and Myc–p53 in combinations as indicated. At 30 h post-transfection, p53 was immunoprecipitated before western blotting to detect p53 Ser 46 phosphorylation. IP, immunoprecipitation; IB, immunoblotting; TCL, total cell lysates. (**e**) Inhibition of Axin-induced, p53-dependent apoptosis by Axin^{Fu-NT}. H1299 cells were transfected with different combinations of plasmids as indicated. At 30 h post-transfection, apoptotic cells were counted. Data are mean ± s.e.m., $n = 3$.

the direct p53-binding (MID) domain, failed to show such a dominant-negative effect on Axin-induced p53 Ser 46 phosphorylation (Fig. 1d). Moreover, Axin^{Fu-NT} can form heterodimers with wild-type Axin when co-expressed (Supplementary Information, Fig. S1d). These results indicate that Axin may exert a critical role in preventing tumour formation induced by DNA damage. Apoptosis assays in Axin-null SNU-475 cells or U2OS cells depleted of Axin by siRNA further confirmed that Axin is required for the induction of apoptosis in response to Dox and UV treatment (Supplementary Information, Fig. S1e, f). Furthermore, Axin stimulated the transcription and protein levels of the *p53AIP1* gene, which is known to be induced by p53 phosphorylation on Ser 46 (Supplementary Information, Fig. S1g, h)[13].

To gain further insights into how Axin controls p53 activation, we carried out a yeast two-hybrid screen using the PP2A-binding domain of Axin (amino-acids 501–712) as bait. One of the identified clones encoded Pirh2 (Supplementary Information, Fig. S2a). To confirm the interaction, we performed co-immunoprecipitation using endogenous proteins from U2OS cell lysates, and found that Axin was detected in the immunoprecipitate of Pirh2 (Fig. 2a). GST (glutathione *S*-transferase) pulldown experiments showed that GST–Pirh2, but not GST itself, can directly interact with His–Axin (Fig. 2b). To determine their interacting regions, we generated a series of deletion mutants of Axin and Pirh2 (schematically outlined in Supplementary Information, Fig. S2b, c) and found that amino-acids 506–576 of Axin are necessary for interaction with amino-acids 211–240 of Pirh2. Two-step co-immunoprecipitation indicated that Axin, Pirh2 and p53 could co-exist in the same complex *in vivo* (Fig. 2c). In addition, Pirh2 interactions with Axin and p53 did not seem to interfere with each other, as Pirh2$^{\Delta Axin}$ (a mutant lacking an Axin-binding domain) could interact with p53, and Pirh2$^{\Delta p53}$ (a mutant lacking a p53-binding domain) could interact with Axin (Supplementary

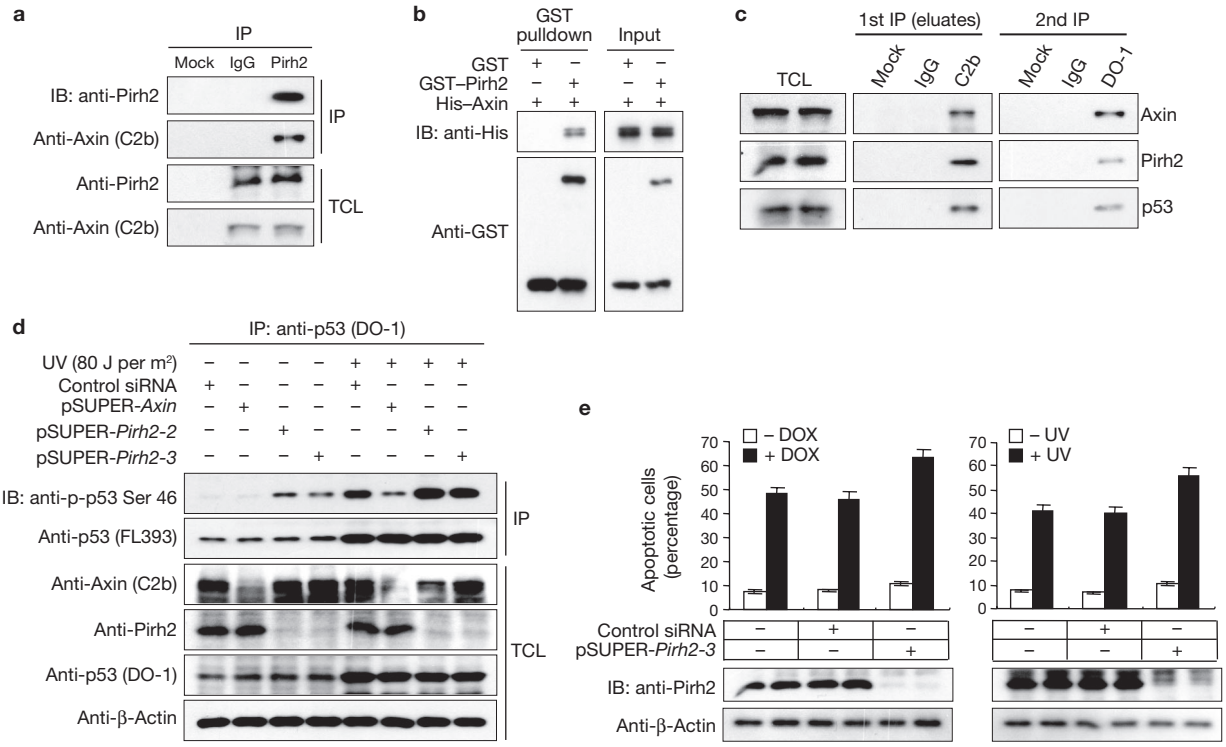

Figure 2 Pirh2 interacts with Axin and inhibits Axin-induced p53 activation and apoptosis. (**a**) U2OS cell lysates were subjected to immunoprecipitation with control IgG or a rabbit anti-Pirh2 polyclonal antibody against endogenous Pirh2. The immunoprecipitates along with total cell lysates were analysed by western blotting with anti-Pirh2 or anti-Axin antibodies. Mock, without lysate. (**b**) Direct interaction between Pirh2 and Axin was determined by a pulldown assay. GST pulldown was performed with His–Axin (2 μg) and GST–Pirh2 (2 μg) or GST as a control. (**c**) Axin, Pirh2 and p53 form a ternary complex. Two-step co-immunoprecipitation was performed using U2OS cell lysates as outlined on the left. It was initally performed using anti-Axin (C2b), followed by elution with the polypeptide against which the C2b antibody was raised (C2b polypeptide). The eluates were subjected to immunoprecipitation with anti-p53 (DO-1) or control IgG before immunoblotting to detect Axin, Pirh2 and p53. (**d**) UV-induced p53 Ser 46 phosphorylation (p-p53 Ser 46) was decreased by knockdown of *Axin*, but increased by knockdown of *Pirh2*. U2OS cells were transfected with pSUPER-*Axin*, pSUPER-*Pirh2* or control siRNA expression vectors. At 30 h post-transfection, cells were irradiated with 80 J m^{-2} UV and collected for immunoprecipitation with DO-1 at 8 h after irradiation. The immunoprecipitates were analysed for total p53 and phosphorylated p53. Total cell lysates were analysed for Axin, Pirh2, p53 and β-actin. (**e**) Knockdown of *Pirh2* increases the rate of apoptosis induced by genotoxic treatment. pSUPER-*Pirh2*-3- or control siRNA-transfected U2OS cells were treated with Dox (2.5 μM; left) or UV (80 J m^{-2}; right) 24 h post transfection. An additional 24 h later, apoptotic cells were counted after Hoechst staining. Data are mean ± s.e.m., $n = 3$. IP, immunoprecipitation; IB, immunoblotting; TCL, total cell lysates.

Information, Fig. S3a, b). For a first approximation, we used ectopically expressed proteins to determine the effect of Pirh2 on Axin-induced p53 Ser 46 phosphorylation. It was found that Pirh2 robustly abrogated p53 phosphorylation, p53 transactivational activity and the induction of apoptosis, which depends on the interaction of p53 with Axin (Supplementary Information, Fig. S3c–e). Pirh2 was unable to inhibit $Axin^{\Delta Pirh2}$-activated p53 Ser 46 phosphorylation or p53 transactivational activity (Supplementary Information, Fig. S3f, g). Knockdown of *Pirh2* in Dox or UV treated U2OS cells led to an increase in p53 Ser 46 phosphorylation (Fig. 2d), protein levels of p53AIP1 (Supplementary Information, Fig. S3h) and in the rate of apoptosis (Fig. 2e).

Pirh2 is characterized by its RING-H2 domain and has been shown to be an E3 ligase towards p53 (ref. 21). We thus assessed the importance of the E3 ligase activity of Pirh2 in its attenuation of Axin-induced p53 phosphorylation. Surprisingly, the $Pirh2^{C145A}$ and $Pirh2^{C164A}$ ligase-dead mutants[21,22] retained the ability to inhibit Axin-induced p53 phosphorylation without altering overall levels of p53 (Fig. 3a). We then performed *in vitro* ubiquitylation assays to determine the E3 activity of Pirh2 towards p53 by using Mdm2 as a positive E3 control, using the protocol described previously[21]. GST–Pirh2 did not show E3 activity towards p53, whereas Mdm2 strongly ubiquitylated p53 (Supplementary Information, Fig. S4a). To investigate further, we included p27 as a positive control for Pirh2 E3 ligase activity[23]. Whereas Pirh2 did indeed show strong E3 activity towards p27 (Supplementary Information, Fig. S4b), it did not show any ubiquitylating activity towards p53. The indistinguishable inhibitory effects of wild-type Pirh2 and its $Pirh2^{C145A}$ mutant on p53 activation were recapitulated in a xenograft tumour growth assay using nude mice (Fig. 3b; Supplementary Information, Fig. S4c, d). In addition, Pirh2 could no longer promote the tumour growth of p53-depleted cells, indicating that Pirh2 stimulates xenograft tumour growth by inhibiting p53 function (Fig. 3b, bottom).

The observation that Pirh2 attenuates Axin-induced p53 Ser 46 phosphorylation independently of its E3 activity prompted us to explore the possibility that Pirh2 might block HIPK2 binding to Axin. Indeed, Pirh2 could compete against HIPK2 for binding to Axin (Supplementary Information, Fig. S4e). We also performed an *in vitro* reconstitution assay, and found that increasing amounts of Pirh2 dissociated HIPK2 from Axin (Supplementary Information, Fig. S4f). Consistently, knockdown of *Pirh2* resulted in higher quantities of HIPK2 co-immunoprecipitated with Axin

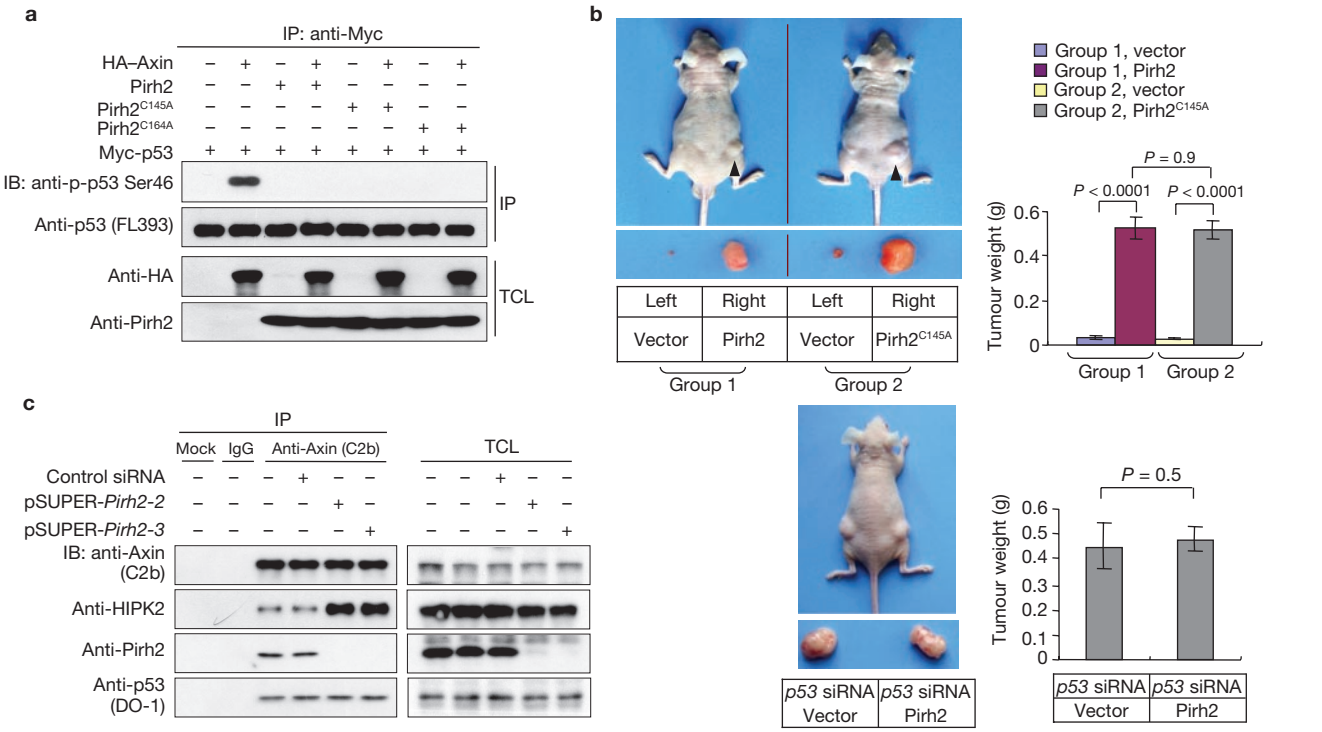

Figure 3 Pirh2 inhibits Axin-induced p53 activation independently of its E3 ligase activity. (**a**) Pirh2 and its ligase-dead mutants, Pirh2^{C145A} and Pirh2^{C164A}, effectively inhibit p53 Ser 46 phosphorylation. H1299 cells were cotransfected with the indicated combinations of HA-Axin, Pirh2, Pirh2^{C145A}, Pirh2^{C164A} and Myc–p53, before p53 Ser 46 phosphorylation levels were determined. Pirh2^{C145A} and Pirh2^{C164A} inhibited Axin-induced p53 Ser 46 phosphorylation as effectively as wild-type Pirh2. (**b**) Top, Pirh2^{C145A} promotes xenograft tumour growth in nude mice as effectively as wild-type Pirh2. Data are mean ± s.e.m., $n = 3$, Student's *t*-test. Bottom, Pirh2 promotes tumour growth by suppressing p53 function. The endogenous p53 in U2OS cells was knocked down by siRNA, and growth of the cells was not affected by Pirh2. Data are mean ± s.e.m., $n = 3$, Student's *t*-test. (**c**) Knockdown of *Pirh2* by pSUPER-*Pirh2*-2 or pSUPER-*Pirh2*-3 results in higher levels of HIPK2 co-immunoprecipitated with Axin. U2OS cells were transfected with pSUPER-*Pirh2*-2, pSUPER-*Pirh2*-3 or control siRNA and their cell lysates were subjected to immunprecipitation with a rabbit anti-Axin antibody (C2b, for endogenous Axin) or IgG as a control. Immunoprecipitates were analysed for Axin, HIPK2, Pirh2 and p53. IP, immunoprecipitation; IB, immunoblotting; TCL, total cell lysates.

(Fig. 3c). In parallel, as Tip60 has been implicated in the regulation of p53 activity under genotoxic stress[24–26], we tested whether Axin also interacted with Tip60 and found that Tip60 was readily detected in the immunoprecipitate by an anti-Axin antibody (Fig. 4a). GST pulldown experiments showed that Axin directly interacts with Tip60 (Fig. 4b). Two-step co-immunoprecipitation using endogenous proteins revealed that Tip60 forms a ternary complex with Axin and p53 (Supplementary Information, Fig. S5a). Notably, the Pirh2-binding domain of Axin (amino-acids 507–576) also interacts with Tip60 (amino-acids 259–389; Supplementary Information, Fig. S5b, c). We therefore tested whether Tip60 might affect Pirh2 binding to Axin. As shown in Fig. 4c, when Tip60 was co-expressed, Pirh2 co-precipitation with Axin was decreased, indicating that Tip60 and Pirh2 are mutually exclusive in their binding to Axin. In addition, an acetyltransferase-dead form of Tip60 (mutant Q377E/G380E, Tip60^{ATD}) excluded Pirh2 from Axin as efficiently as wild-type Tip60, indicating that it is unlikely that the enzymatic activity of Tip60 is involved in its competion with Pirh2 for Axin interaction. An *in vitro* reconstitution assay also confirmed the competitive binding between Tip60 and Pirh2 to Axin (Supplementary Information, Fig. S5d).

The diversity of complexes centred on Axin led us to explore whether such distinct complexes are formed in cells in response to differing severities of genotoxic insults. We treated cells with varying doses of Dox (Supplementary Information, Fig. S6a, b); 0.4 μM and 2.5 μM were the doses required for U2OS cells to undergo cell-cycle arrest and apoptosis, respectively. We then carried out immunoprecipitation to analyse complex formation among endogenous Axin, Pirh2 and Tip60 after sublethal or lethal drug treatment. A higher level of Pirh2 was co-precipitated with Axin in cells treated with the sublethal dose of Dox than in lethal dose-treated cells. In contrast, a higher amount of Tip60 was co-precipitated with Axin in the lethal dose-treated cells, despite the relatively unchanged protein levels of Pirh2 and Tip60 (Fig. 4d). In the same experiment, it was also found that higher levels of p53 were associated with Axin than in untreated cells, irrespective of sublethal or lethal treatment (probably due to increased p53 levels as a result of the Dox treatment) and that more HIPK2 was associated with Axin on lethal treatment, which is in accordance with the competitive nature of Pirh2 and HIPK2 in binding to Axin. Higher levels of Tip60 and lower levels of Pirh2 associated with Axin were also seen in cells treated with a lethal dose of UV (80 J m^{-2}) than in cells treated with a sublethal dose (10 J m^{-2}; Supplementary Information, Fig. S6c). Furthermore, in lethally treated cells depleted of Tip60 by siRNA, levels of Pirh2 co-precipitated with Axin were as high as those in sublethally treated cells, highlighting the importance of the competitive nature of Tip60 and Pirh2 binding in cells that are exposed to lethal radiation (Fig. 4e). To observe the dynamic interactions among Axin, p53, Pirh2 and Tip60 at their endogenous levels *in vivo*, we performed a series of immunostaining experiments. Axin interaction with p53 in the nucleus was increased under UV lethal treatment, concomitant with an increase in levels of nuclear Axin and p53 (Supplementary Information, Fig. S7). Axin interacts with Pirh2 in both

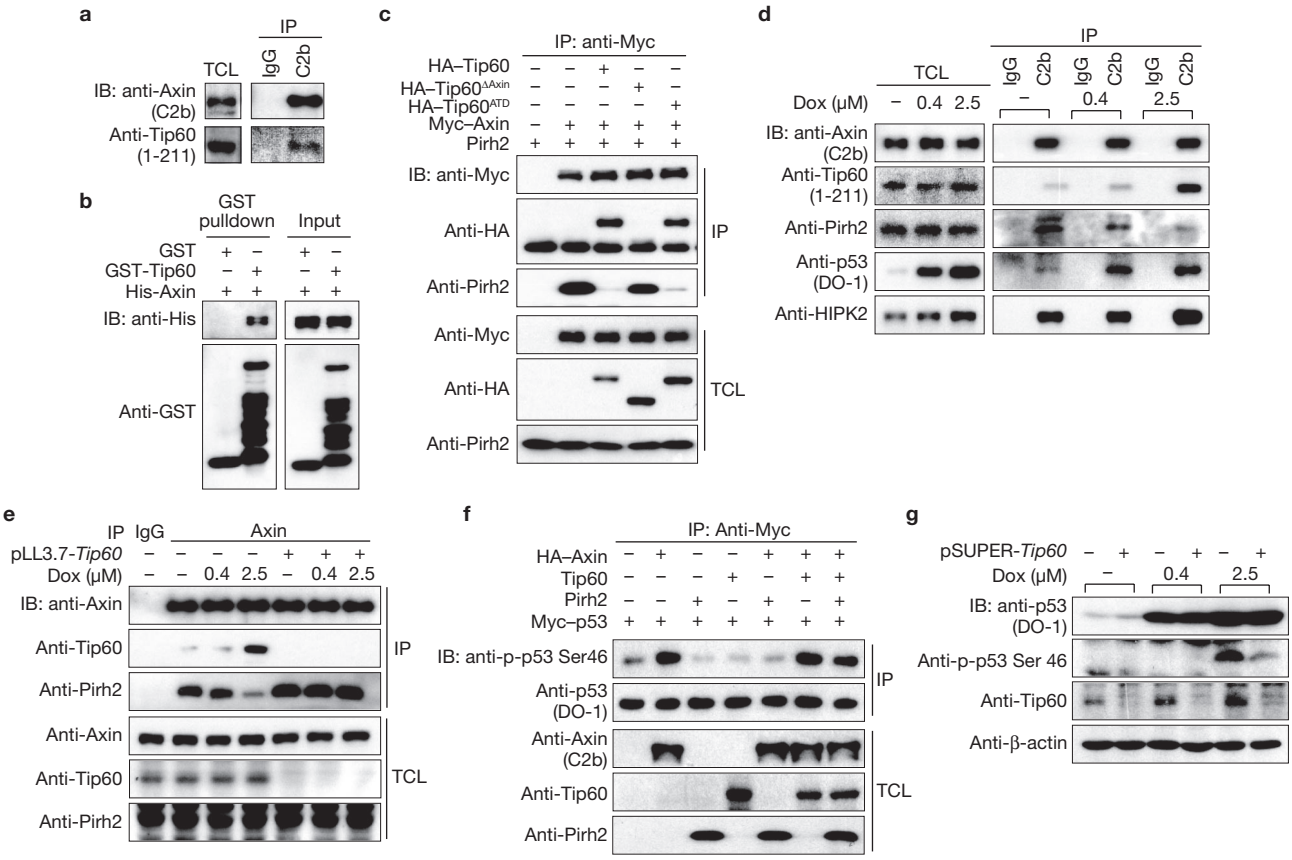

Figure 4 Tip60 interacts with Axin and reverses Pirh2 inhibition of p53. (**a**) U2OS cell lysates were subjected to immunoprecipitation with control IgG or an anti-Axin antibody (C2b), before western blotting with anti-Tip60 (1-211) and anti-Axin antibodies. (**b**) Direct interaction between Tip60 and Axin determined by a pulldown assay. GST pulldown was performed with His–Axin (2 μg) and GST–Tip60 (2 μg) or GST as a control. (**c**) Tip60 and Tip60^{ATD} (acetyltransferase dead), but not Tip60$^{\Delta Axin}$ (which lacks the Axin-binding domain), prevent Pirh2 from binding to Axin. Myc–Axin, Pirh2, HA–tagged Tip60, Tip60$^{\Delta Axin}$ or Tip60^{ATD} were co-transfected in different combinations as indicated. Myc–Axin was immunoprecipitated, before precipitates were analysed for Tip60 and Pirh2. Tip60$^{\Delta Axin}$ failed to dissociate Pirh2 from Axin. (**d**) Decreased Pirh2–Axin and increased Tip60–Axin interactions on treatment with a lethal dosage of Dox. U2OS cells were untreated or treated with Dox (0.4 μM or 2.5 μM) for 18 h, before immunoprecipitation with anti-Axin (C2b). Immunoprecipitates and total cell lysates were analysed for Axin, Pirh2, Tip60, p53 or HIPK2. (**e**) Knockdown of *Tip60* leads to increased amounts of Axin-associated Pirh2 on treatment with a lethal dosage of Dox. U2OS cells depleted of Tip60 were untreated or treated with Dox (0.4 μM or 2.5 μM) for 18 h, before immunoprecipitation with anti-Axin (C2b). Immunoprecipitates and total cell lysates were analysed for Axin, Pirh2 and Tip60. (**f**) Tip60 reverses Pirh2 attenuation of Axin-induced p53 activation. H1299 cells were transfected with HA–Axin, Tip60, Pirh2 and Myc-p53 in the combinations indicated. Cells were lysed and immunoprecipitated with an anti-Myc antibody at 24 h post-transfection, followed by analysis with the indicated antibodies. (**g**) Knockdown of *Tip60* decreased the p53 Ser 46 phosphorylation induced by treatment with a lethal dose of Dox. At 24 h after transfection with control siRNA or pSUPER-*Tip60*, U2OS cells were untreated or treated with Dox (0.4 μM or 2.5 μM) for 18 h. Cells were then lysed and subjected to western blotting with the indicated antibodies. IP, immunoprecipitation; IB, immunoblotting; TCL, total cell lysates.

the nucleus and cytoplasm of untreated and sublethally treated cells, but their co-staining was decreased in lethally treated cells (Supplementary Information, Fig. S8). Tip60 colocalized to Axin in perinuclear cytoplasmic areas in untreated or sublethally treated cells, and in the nucleus after lethal treatment (Supplementary Information, Fig. S9). A triple co-staining experiment confirmed that Axin, p53 and Tip60 are most prominently colocalized in the nucleus in response to lethal UV treatment (Supplementary Information, Fig. S10).

We next determined the effects of Tip60 on Axin-induced p53 activity. Consistent with competitive binding of Tip60 against Pirh2 to Axin, Tip60 could reverse the inhibition by Pirh2 of Axin-induced p53 activation, including phosphorylation at Ser 46 (Fig. 4f) and p53 transactivational activity (Supplementary Information, Fig. S11a). We further addressed the physiological roles of Tip60 in U2OS cells in response to sublethal or lethal treatment with Dox. Knockdown of *Tip60* resulted in decreased p53 Ser 46 phosphorylation on lethal Dox treatment (Fig. 4g). The ability of Tip60 to reverse the inhibitory effect of Pirh2 on Axin-induced growth inhibition was confirmed by a colony formation assay (Supplementary Information, Fig. S11b). We also found that Tip60 depletion reduced the number of cells undergoing apoptosis induced by lethal DNA damage (Supplementary Information, Fig. S11c). We further tested the effects of *Axin*, *Pirh2* or *Tip60* knockdown on cell-cycle progression, and found that it was not affected in untreated cells or cells sublethally treated with Dox, consistent with our previous assertion that Axin does not activate p53 transactivational activity on p21 (cyclin-dependent kinase inhibitor 1A, which mediates the p53-dependent cell-cycle G1 phase arrest; Supplementary Information, Fig. S11d, e)[17,18].

We attempted to delineate the signalling pathways that dictate different complex formation according to DNA damage severity, and found that ATM (ataxia telangiectasia mutated) and ATR (ATM and

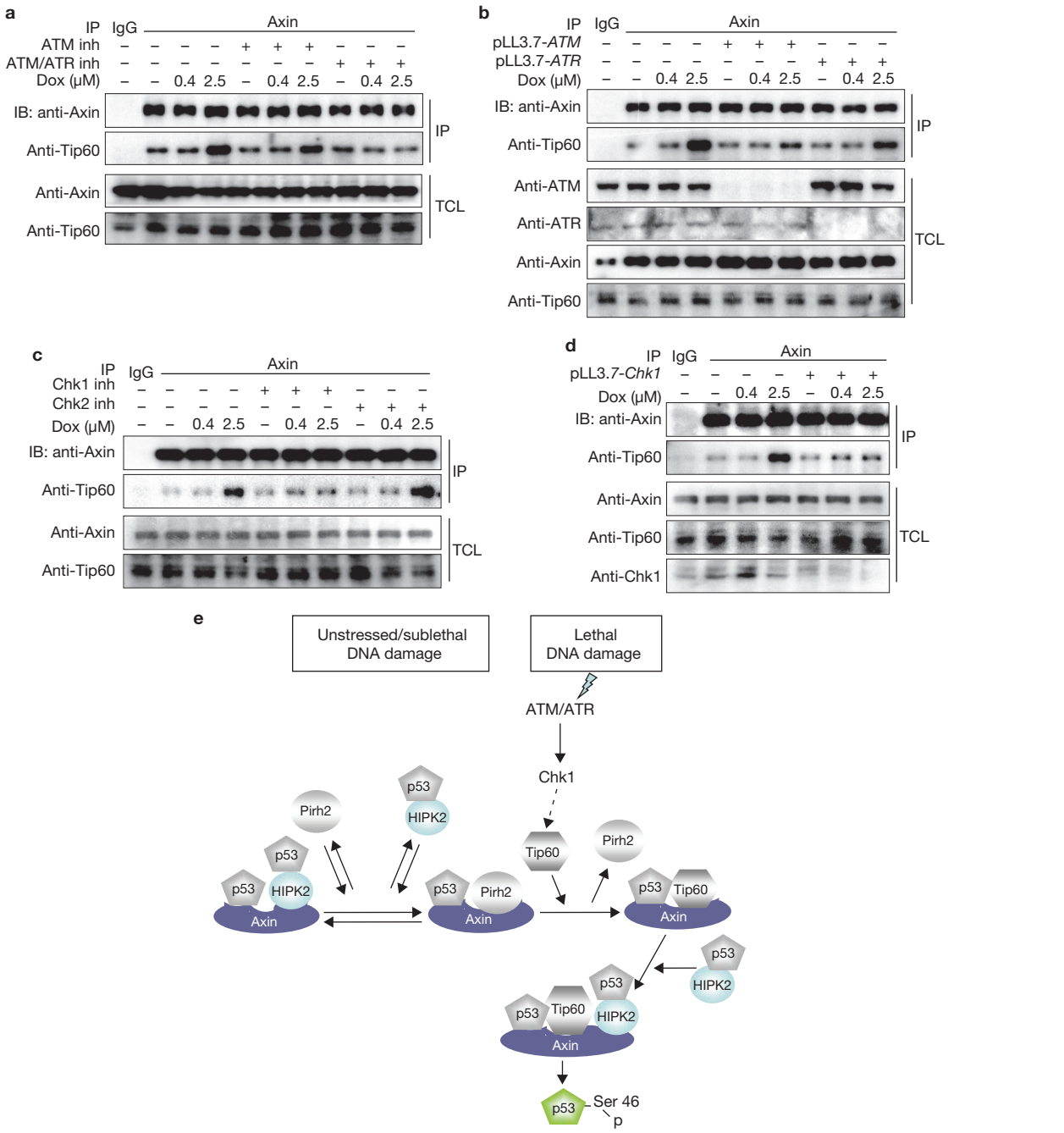

Figure 5 ATM, ATR and Chk1 are involved in Tip60-enriched p53 activating complex centred on Axin. (**a**) U2OS cells were pretreated with DMSO alone, DMSO containing an ATM and ATR inhibitor (inh; 5 μM) or DMSO containing an inhibitor for ATM only (10 μM) for 1 h before treatment with Dox (0.4 μM or 2.5 μM) for 18 h, followed by immunoprecipitation using an anti-Axin (C2b) antibody. Western blotting of the precipitates was performed with anti-Axin and anti-Tip60 (1-211) antibodies. (**b**) Knockdown of *ATM* and *ATR* abolishes the increase in Tip60–Axin interaction on treatment with a lethal dose of Dox. U2OS cells were infected with lentiviral pLL3.7-control siRNA, pLL3.7-*ATM* or pLL3.7-*ATR*. Cells were left untreated or treated with Dox (0.4 μM or 2.5 μM) for 18 h, before immunoprecipitation with an anti-Axin (C2b) antibody. The immunoprecipitates and total cell lysates were analysed with the antibodies indicated. (**c**) Inhibition of Chk1 abolished the increase in Tip60–Axin interaction in cells treated with a lethal dose of Dox. U2OS cells were pretreated with a Chk1 (5 μM) or Chk2 (1 μM) inhibitor for 1 h before treatment with Dox (0.4 μM or 2.5 μM). At 18 h post-treatment, cell lysates were immunoprecipitated with an anti-Axin (C2b) antibody, followed by western blotting with anti-Axin and anti-Tip60 (1-211) antibodies. (**d**) Knockdown of *Chk1* abolishes the increase in Tip60–Axin interaction. U2OS cells were infected with lentiviral control siRNA or pLL3.7-*Chk1*. Cells were left untreated or treated with Dox (0.4 μM or 2.5 μM) for 18 h, followed by immunoprecipitation using an anti-Axin antibody. The immunoprecipitates and total cell lysates were analysed with the antibodies indicated. (**e**) A simplified model shows that Axin coordinates the functions of HIPK2, Pirh2 and Tip60 to modulate the activity threshold of p53. The left shows that in normal or sublethally damaged cells the Axin–p53 complex is primarily occupied by Pirh2, such that the complex is devoid of the activating kinase HIPK2. However, on exposure to lethal damage (right), Tip60 is activated by ATM/ATR through Chk1 and subsequently binds to Axin, leading to dissociation of Pirh2 from Axin and allowing the formation of a complex consisting of Axin, HIPK2, p53 and Tip60 that leads to maximal activation of p53 through phosphorylation at Ser 46, which ultimately triggers apoptosis. IP, immunoprecipitation; IB, immunoblotting; TCL, total cell lysates.

Rad3-related; both DNA-damage sensors) are involved. In U2OS cells, although an inhibitor of ATM alone mildly reduced the level of Axin-bound Tip60 under lethal Dox treatment, an inhibitor of both ATM and ATR caused a far greater decrease in Tip60 co-immunoprecipitated with Axin (Fig. 5a). Furthermore, knockdown of *ATM* or *ATR* dampened the increase of Axin–Tip60 interaction after lethal DNA damage (Fig. 5b). These results indicate that ATM and ATR kinases can impinge on the Axin–Tip60 complex formation, further linking Axin to the genotoxic response cascade. It should be noted that although ATM and ATR could also be activated on sublethal DNA damage, they did not alter Axin–Tip60 interaction, compared with untreated cells. A possible explanation is that the pro-apoptotic Axin–Tip60 complex formation may require higher kinase activity levels and/or that the kinases have different subcellular localizations or binding partners under different conditions. As recent reports have shown, HIPK2 activity can be modulated by ATM and ATR[27], we considered whether HIPK2 could modulate the affinity of Pirh2 and Tip60 for Axin. However, as shown in Supplementary Information, Fig. S11f, *HIPK2* knockdown had no impact on Tip60–Axin interaction. To investigate further, we tested whether Chk1 and Chk2 (cell-cycle checkpoint kinases 1 and 2, ATM and ATR substrates) are involved in the regulation of Axin–Tip60 interaction on lethal DNA treatment. We found that Chk1, but not Chk2, is necessary to elevate Axin–Tip60 interaction (Fig. 5c, d), emphasizing the link between the ATM and ATR signalling cascade and Axin-mediated apoptosis in response to lethal DNA damage.

This study reports two interacting partners for Axin, Pirh2 and Tip60, and a new Axin-centred regulatory circuitry for fine-tuning the p53 activition threshold in response to differing severities of genotoxic stress. In non-severely damaged cells, Pirh2 interacts with Axin and causes dissociation of HIPK2 from Axin (Fig. 5e), suggesting that in these cells HIPK2 does not participate in p53 Ser 46 phosphorylation. In fact, our study is consistent with the finding that in non-severely damaged cells, HIPK2 is degraded by Mdm2 (ref. 9). Under lethal doses of genotoxic stress, ATM and ATR activate Tip60, enabling it to interact with the Axin–HIPK2–p53 activation complex by excluding the inhibiting Pirh2 to elicit an irreversible apoptotic process that eliminates severely damaged cells. This unifies the critical roles of HIPK2 and Tip60 in the induction of apoptosis on lethal DNA damage. A carcinogenesis-induction experiment using the $Axin^{Fu}$/+ mouse cell line has uncovered that Axin is a latent tumour suppressor; we further suggest that Axin may be prototypic of a great number of latent regulatory factors whose deletion or truncation mutants do not show apparent phenotypes in mice unless triggered by genotoxins or other stress signals. □

METHODS

Methods and any associated references are available in the online version of the paper at http://www.nature.com/naturecellbiology/.

Note: Supplementary Information is available on the Nature Cell Biology website.

ACKNOWLEDGEMENTS

This work was supported by grants from the 973 Program and 863 Program (2007CB914602, 2006CB503900 and 2006AA02A303), the National Natural Science Foundation of China (30730025, 30871280 and 30770454), the Ministry of Education of China (705030 and B06016), the National Basic Research Program of the Ministry of Science and Technology and the National Science Foundation of Fujian Province (2009J06021). We thank H. You for commenting on the manuscript.

AUTHOR CONTRIBUTIONS

Q.L., S.L. and S.C.L. conceived and designed the study. Q.L., S.L., X.W., G.L., Z.L., H.G. and R.K. performed the research; Y.W., Z.Y. and J.H. helped with data analysis and Q.L., S.L. and S.C.L. wrote the paper.

COMPETING FINANCIAL INTERESTS

The authors declare no competing financial interests.

Published online at http://www.nature.com/naturecellbiology/.
Reprints and permissions information is available online at http://npg.nature.com/reprintsandpermissions/.

1. Riley, T., Sontag, E., Chen, P. & Levine, A. Transcriptional control of human p53-regulated genes. *Nature Rev. Mol. Cell Biol.* **9,** 402–412 (2008).
2. Masha, V., Poyurovsky & Prives, C. Unleashing the power of p53: lessons from mice and men. *Genes Dev.* **20,** 125–131 (2006).
3. Vousden, K. H. & Lu, X. Live or let die: the cell's response to p53. *Nature. Rev. Cancer* **8,** 594–604 (2002).
4. Dey, A., Verma, C. S. & Lane, D. P. Updates on p53: modulation of p53 degradation as a therapeutic approach. *Br. J. Cancer* **98,** 4–8 (2008).
5. Oren, M. Decision making by p53: life, death and cancer. *Cell Death Differ.* **4,** 431–442 (2003).
6. Harper, J. W. & Elledge, S. J. The DNA damage response: ten years after. *Mol. Cell* **28,** 739–745 (2007).
7. D'Orazi, G. *et al.* Homeodomain-interacting protein kinase-2 phosphorylates p53 at Ser-46 and mediates apoptosis. *Nature Cell Biol.* **4,** 11–19 (2002).
8. Hofmann, T. G. *et al.* Regulation of p53 activity by its interaction with homeodomain-interacting protein kinase-2. *Nature Cell Biol.* **4,** 1–10 (2002).
9. Rinaldo, C. *et al.* MDM2-regulated degradation of HIPK2 prevents p53 Ser46 phosphorylation and DNA damage-induced apoptosis. *Mol. Cell* **9,** 739–750 (2007).
10. Gresko, E. *et al.* Autoregulatory control of the p53 response by caspase-mediated processing of HIPK2. *EMBO J.* **25,** 1883–1894 (2006).
11. Oda, K. *et al.* p53AIP1, a potential mediator of p53-dependent apoptosis, and its regulation by Ser-46-phosphorylated p53. *Cell* **102,** 849–862 (2000).
12. Polakis, P. The many ways of Wnt in cancer. *Curr. Opin. Genet. Dev.* **17,** 45–51 (2007).
13. Zeng, L. *et al.* The mouse *Fused* locus encodes Axin, an inhibitor of the Wnt signaling pathway that regulates embryonic axis formation. *Cell* **90,** 181–192 (1997).
14. Inoki, K. *et al.* TSC2 integrates Wnt and energy signals via a coordinated phosphorylation by AMPK and GSK3 to regulate cell growth. *Cell* **126,** 955–68 (2006).
15. Rui, Y. *et al.* A β-catenin-independent dorsalization pathway activated by Axin/JNK signaling and antagonized by Aida. *Dev. Cell* **13,** 268–82 (2007).
16. Wan, M. *et al.* Parathyroid hormone signaling through low-density lipoprotein-related protein 6. *Genes Dev.* **21,** 2968–2979 (2008).
17. Rui, Y. *et al.* Axin stimulates p53 functions by activation of HIPK2 kinase through multimeric complex formation. *EMBO J.* **23,** 4583–4594 (2004).
18. Li, Q. *et al.* Daxx cooperates with the Axin/HIPK2/p53 complex to induce cell death. *Cancer Res.* **67,** 66–74 (2007).
19. Lu, Z. *et al.* Protein encoded by the Axin (*Fu*) allele effectively down-regulates Wnt signaling but exerts a dominant negative effect on c-Jun N-terminal kinase signaling. *J. Biol. Chem.* **283,** 13132–13139 (2008).
20. Sun, P. *et al.* PRAK is essential for ras-induced senescence and tumor suppression. *Cell* **128,** 295–308 (2007).
21. Leng, R. P. *et al.* Pirh2, a p53-induced ubiquitin-protein ligase, promotes p53 degradation. *Cell* **112,** 779–791 (2003).
22. Beitel, L. K. *et al.* Cloning and characterization of an androgen receptor N-terminal-interacting protein with ubiquitin-protein ligase activity. *J. Mol. Endocrinol.* **29,** 41–60 (2002).
23. Hattori, T. *et al.* Pirh2 promotes ubiquitin-dependent degradation of the cyclin-dependent kinase inhibitor p27Kip1. *Cancer Res.* **67,** 10789–10795 (2007).
34. Legube, G. *et al.* Role of the histone acetyl transferase Tip60 in the p53 pathway. *J Biol Chem.* **279,** 44825–44833 (2004).
25. Tang, Y., Luo, J., Zhang, W. & Gu, W. Tip60-dependent acetylation of p53 modulates the decision between cell-cycle arrest and apoptosis. *Mol. Cell* **24,** 827–839 (2006).
26. Sykes, S. M. *et al.* Acetylation of the p53 DNA-binding domain regulates apoptosis induction. *Mol. Cell* **24,** 841–851 (2006).
27. Winter, M., Sombroek, D., Dauth, I., Moehlenbrink, J., Scheuermann, K., Crone, J. & Hofmann, T. G. Control of HIPK2 stability by ubiquitin ligase Siah-1 and checkpoint kinases ATM and ATR. *Nature Cell Biol.* **10,** 812–824 (2008).

METHODS

Plasmid constructions. Full-length cDNA encoding mouse Pirh2 was obtained by PCR using mouse testis cDNA. Point mutations of Pirh2 were generated by a PCR-based site-directed mutagenesis method using Pfu polymerase (Stratagene). Full-length cDNA encoding human Tip60 was obtained from an EST clone (IMAGE No. 601205534, Invitrogen). All expression plasmids were constructed in the pCMV5 vector. PCR products were verified by sequencing (Invitrogen). The details of the primer sequences used for point mutations and deletion mutations are available on request. The various constructs of Axin, HIPK2 and p53 were as described previously[15].

RNA interference. The mammalian expression vector pSUPER or lentiviral based vector pLL3.7 were used for expression of siRNA in U2OS cells. All pSUPER-based interfering plasmids were constructed by inserting a 19-nucleotide sequence corresponding to a specific transcribed region of a target gene, as described previously[28]. The 19-nucleotide sequences of *Pirh2* targeted by pSUPER-*Pirh2*-1, pSUPER-*Pirh2*-2 and pSUPER-*Pirh2*-3 are 5′-CTAGATCGCTTTAAAGTGA-3′, 5′-TGCCGCTTGTGTCATGATA-3′ and 5′-CAATGAAG ATCATCAACTA-3′, respectively. The sequence targeting *p53* in pSUPER-p53 is 5′-GACTCCA GTGGTAATCTAC-3′; sequences for pSUPER-*Axin* and pSUPER-*HIPK2* are as described previously[17]. Control siRNA was expressed by the pSUPER vector carrying a 19-nucleotide scrambled sequence (5′-TCCTACAAATTCCACAGTT-3′). The sequences of *Tip60* targeted by pSUPER-*Tip60* and by pLL3.7-*Tip60* are 5′-CGTCTGGATGAATGGGTGA-3′ and 5′-GAACCAGGACAACGAAGAT-3′, respectively. The 19-nucleotide sequence of *Axin* targeted by pLL3.7-*Axin* is 5′-GGAGAAGATCATCGGCAA-3′; the sequences for *ATM* and *ATR* in pLL3.7 are 5′-GAAGGAAGCCAGAGTACAA-3′ and 5′-GGTCAGCTGTCTACTGTTA-3′, respectively. The 19-nucleotide sequence of *Chk1* targeted by pLL3.7-*Chk1* was 5′-GCGTGCCGTAGACTGTCCA-3′.

Antibodies and drugs. Rabbit polyclonal anti-Axin antibodies C2b and C8b were raised as described previously[17]. Mouse anti-HA (F-7), anti-Myc (9E10), anti-p53 (DO-1), anti-p53 (FL393), anti-Axin (S-20), anti-HIPK2 (C-15), anti-Pirh2 (T-18), anti-Tip60 (N-17) and anti-Chk1 (G-4) antibodies were from Santa Cruz Biotechnology, Inc. The mouse anti-Flag (M2) antibody was from Sigma. The rabbit polyclonal phospho-p53^{Ser-46} antibody was from Cell Signaling Technology. The rabbit polyclonal anti-Pirh2 (CA1012) antibody was from Calbiochem. The Tip60 antibody was from Upstate (Cat. No. 07-038). The mouse polyclonal antibody against Tip60 (1-211) was generated by immunizing mice with a GST-fusion protein containing amino-acids 1–211 of human Tip60. The rabbit polyclonal antibody against Tip60 (M) was generated by immunizing rabbits with a GST-fusion protein containing amino-acids 149–250 of human Tip60. Antibodies against p53AIP1 (ab3678) were from Abcam. Antibodies against ATM (Ab-3) and ATR (Ab-2) were from Calbiochem. Doxorubicin was from Sigma (Cat. No. D44583). The ATM/ATR (Cat. No. 118501), ATM (Cat. No. 118500), Chk1/Wee1 (Cat. No. 681637) and Chk2 (Cat. No. 220485) inhibitors were from Calbiochem. Blasticidin was from InvivoGen (Cat. No. ant-bl-5b). All primary antibodies for immunoblotting were used at a 1:1,000 dilution, except for anti-Pirh2 (1:10,000) and anti-ATM (1:100).

Cell culture, transient transfection, immunopreciptation and western blotting. H1299 and U2OS cells were maintained in Dulbecco's modified Eagle's medium (DMEM) supplemented with 10% fetal bovine serum, 2 mM L-glutamine, 100 IU penicillin and 100 mg ml^{-1} streptomycin at 37°C in a humidified incubator containing 5% CO2. Mouse skin fibroblasts were obtained from *Axin*^{Fu}/+ or +/+ mice by trypsin digestion of the mouse skin after mincing, and were cultured in DMEM with 10% fetal bovine serum, non-essential amino acids, sodium pyrovate, 2 mM L-glutamine, 100 IU penicillin and 100 mg ml^{-1} streptomycin. Lipofectamine 2000 was used for transfection. Over 90% transfection efficiency was achieved in U2OS and H1299 cells. To ensure an equal amount of total DNA was transfected in each sample, a corresponding empty vector was used for adjustment of total DNA. Transfected cells were collected at 30 h after transfection using a lysis buffer and immunoprecipitation was carried out as described previously[17].

Yeast two-hybrid screening. Yeast two-hybrid screening was carried out using MATCHMAKER GAL4 Two-Hybrid System 3 (Clontech) according to the manufacturer's instructions as described previously[15]. The bait was the PP2A domain (amino-acids 501–712) of mouse Axin.

Transcription reporter assays. The pathDetect p53-Luc reporter that carries p53-specific enhancer elements was from Stratagene. The pGL3-*p53AIP1* luciferase reporter was constructed as described previously[11]. H1299 cells were transiently transfected with p53-Luc reporter (0.5 μg) and a trace amount of p53 (10 ng) along with other plasmids in different combinations. Each sample was supplemented with pCMV5-LacZ (0.5 μg), which expresses β-galactosidase, for monitoring the transfection efficiency. Where necessary, the total amount of transfected DNA in each plate was adjusted to 4 μg with the empty vector pCMV5. At 24 h after transfection, cells were collected and luciferase activity was measured, and presented as described previously[18]. β-galactosidase activity was measured by a spectrophotometer and used for normalization of the luciferase activity data. The results are presented as mean. ± s.e.m. from at least three independent experiments.

Immunofluorescence staining. U2OS cells grown on 22-mm^2 coverslips in six-well plates were washed once with PBS and fixed with 4% formaldehyde in PBS for 10 min at room temperature. Cells were then rinsed with PBS, before being treated with PBS, 0.2% Triton X-100, 2 mg ml^{-1} BSA and 1 mM NaN_3 on ice for 10 min. The coverslips were then incubated with PBS, 0.02% Triton X-100, 3% BSA and 1 mM NaN_3 for 30 min. Cells were then incubated with 2 μg ml^{-1} anti-Axin (S-20), anti-p53 (DO-1) anti-Pirh2 (CA1012) or anti-Tip60 (M) in blocking solution for 30 min. Next, cells were washed four times with PBS, 0.02% Triton X-100, 1.5% BSA and 1 mM NaN_3; incubated with 20 μg ml^{-1} of bovine anti-goat Texas red (Santa Cruz), goat anti-mouse FITC (Santa Cruz), bovine anti-rabbit FITC (Santa Cruz) or goat anti-rabbit Alexa Fluor 647 (Invitrogen) in blocking solution for 30 min. Cells were then washed four times with PBS, 0.02% Triton X-100, 1.5% BSA and 1 mM NaN_3 before being incubated with DAPI (1 μg ml^{-1}) in washing solution for 2 min. Specimens were mounted in 90% glycerol and sealed with nail polish.

Two-step co-immunoprecipitation. Two-step co-immunoprecipitation was performed essentially according to the procedures described previously[29]. Briefly, U2OS cells were lysed with LSLD buffer, sonicated and centrifuged. The supernatant was subjected to immunoprecipitation by incubating with an anti-Axin antibody (C2b) bound to Protein A/G-agarose beads for 2 h at 4 °C. The beads were washed with lysis buffer containing NaCl (150 mM) three times, and the Axin-based protein complexes were eluted with lysis buffer (300 μl) containing NaCl (250 mM) and C2b antigen (100 μg ml^{-1}) for 2 h at 4°C. The second immunoprecipitation was performed using eluate (150 μl) from the first immunoprecipitate and lysis buffer (350 μl) containing NaCl (150 mM) and an anti-p53 antibody (1 μg; DO-1) or a control IgG. The immunoprecipitates were then anlysed with indicated antibodies.

Tumorigenesis assays. Inbred 129P4/RrRk *Axin*^{Fu}/+ mice (Jackson Lab.) were maintained and genotyped as described previously[19]. Littermates from heterozygous parents were treated with 0.5% DMBA (50 μl) in acetone on the dorsal posterior surface on postnatal day 2. One week later, the mice were further treated with 6.25 μg of TPA in 100 μl acetone twice a week for a total of 12 weeks. Papilloma and normal skin sections from wild-type and *Axin*^{Fu}/+ mice were fixed in 10% PBS-buffered formaldehyde and stained with hematoxylin and eosin. Images were taken with an Olympus microscope at various magnifications.

Xenograft tumour assays. For tumour formation in nude mice, pcDNA6.0, which harbours a blasticidin-resistant gene, was included in each transfection. After transfection, cells were selected with blasticidin (10 μg ml^{-1}) and the resistant cells (5×10^6 cells in 100 μl DMEM per injection) were injected subcutaneously into the flanks of nude mice. Six weeks later, tumours were removed and weighed.

28. Brummelkamp, T. R., Bernards, R. & Agami, R. A system for stable expression of short interfering RNAs in mammalian cells. *Science* **296,** 550–553 (2002).
29. Harada, J. *et al.* Requirement of the co-repressor homeodomain-interacting protein kinase 2 for ski-mediated inhibition of bone morphogenetic protein-induced transcriptional activation. *J. Biol. Chem.* **278,** 38998–39005 (2003).

nature cell biology

DOI: 10.1038/ncb1927

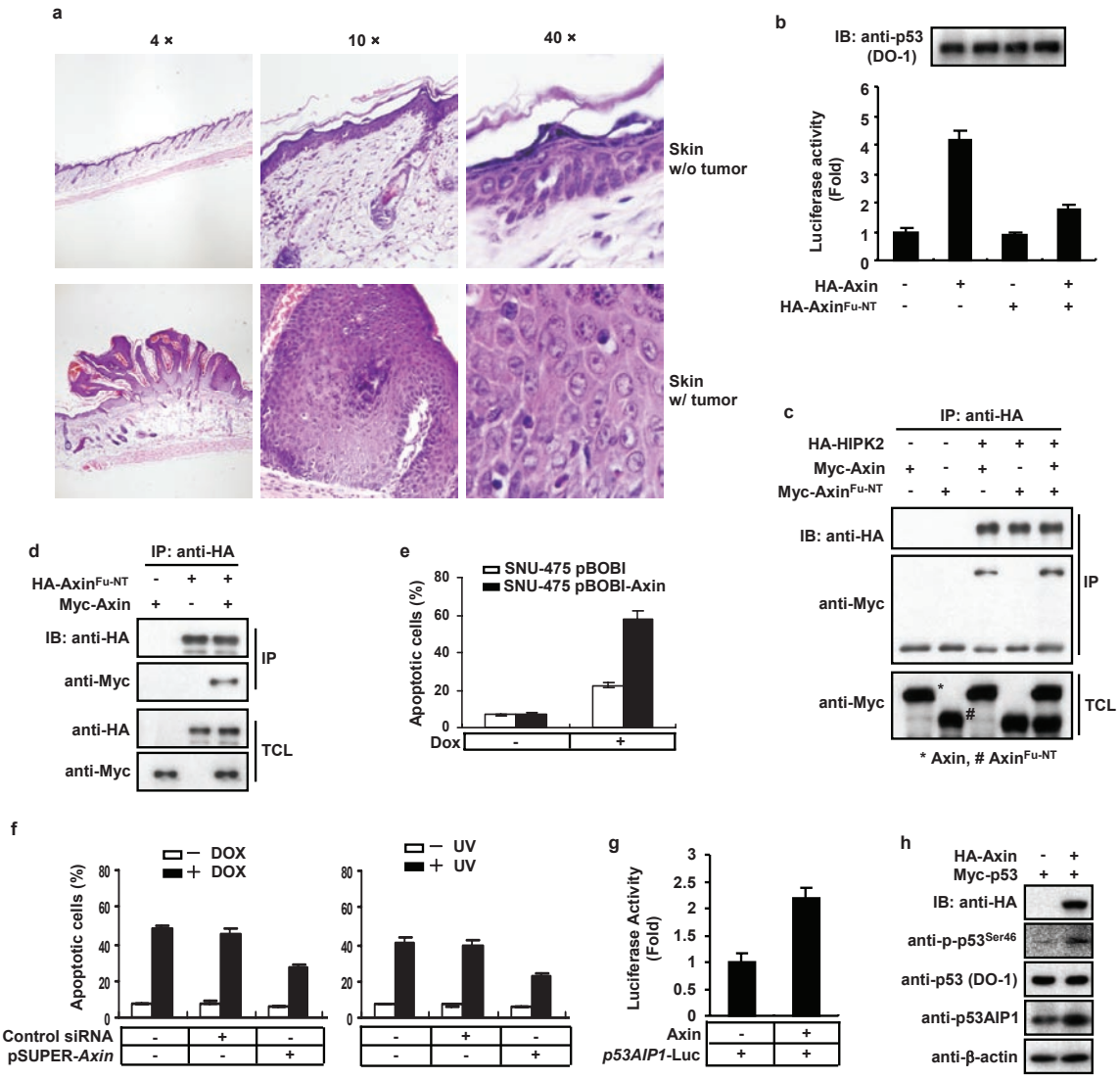

Figure S1 The molecular mechanism underlying the increased tumorigenesis in the mutant mice. **(a)** Normal skin and tumor tissues from DMBA-treated wildtype and $Axin^{Fu}$/+ mice were fixed in 10% formalin overnight and sectioned at 7 μm followed by staining with hematoxylin and eosin. Shown are representative images taken at ×4, ×10 and ×40 amplifications with an Olympus microscope. **(b)** Axin$^{Fu\text{-}NT}$ has a dominant negative effect on Axin-stimulated transcriptional activity of the p53-luciferase reporter gene. H1299 cells were co-transfected with Axin or Axin$^{Fu\text{-}NT}$ together with p53-Luc and trace amount of p53. Luciferase activities were measured. The results were normalized to the activity of LacZ and are presented as means±s.e.m. of five separate experiments. **(c)** The Axin$^{Fu\text{-}NT}$ protein does not bind to HIPK2. U2OS cells were co-transfected with HA-HIPK2 and Myc-Axin or Axin$^{Fu\text{-}NT}$ and immunoprecipitation was carried out with anti-HA for HIPK2, followed by western blotting to detect Axin. **(d)** Axin$^{Fu\text{-}NT}$ interacts with wildtype Axin. HA-tagged Axin$^{Fu\text{-}NT}$ was cotransfected with Myc-tagged wildtype Axin into U2OS cells. Immunoprecipitation was performed using anti-HA antibody, followed by western blotting using anti-HA or anti-Myc. **(e)** Axin null SNU475 cells infected with pBOBI vector (as a control) or Axin were exposed to 2.5 μM Dox (doxorubicin). At 30 h post treatment, cells were fixed and stained with Hoechst, apoptotic cells were counted. Error bars, s.e.m.; n=3. Reintroduction of Axin in SNU-475 cells by pBOBI-Axin resulted in higher apoptotic rate in Dox treated cells. **(f)** pSUPER-*Axin* and control siRNA were separately transfected into U2OS cells. Cells were treated with 2.5 μM Dox (left) or 80 J/m^2 UV (right) 24 h posttransfection. Apoptotic cells were counted after Hoechst 33342 staining. Error bars, s.e.m.; n=3. Knockdown of *Axin* decreased the number of cells undergoing apoptosis upon treatment. **(g)** U2OS cells were transfected with Axin or vector, together with *p53AIP1*-Luc. At 24 h post transfection, luciferase activities were measured and normalized to the activity of LacZ. Error bars, s.e.m.; n=5. **(h)** H1299 cells were transfected with Axin or vector together with 0.5 μg p53. 24 h posttransfection, IB (immunoblotting) was performed to detect the proteins as indicated.

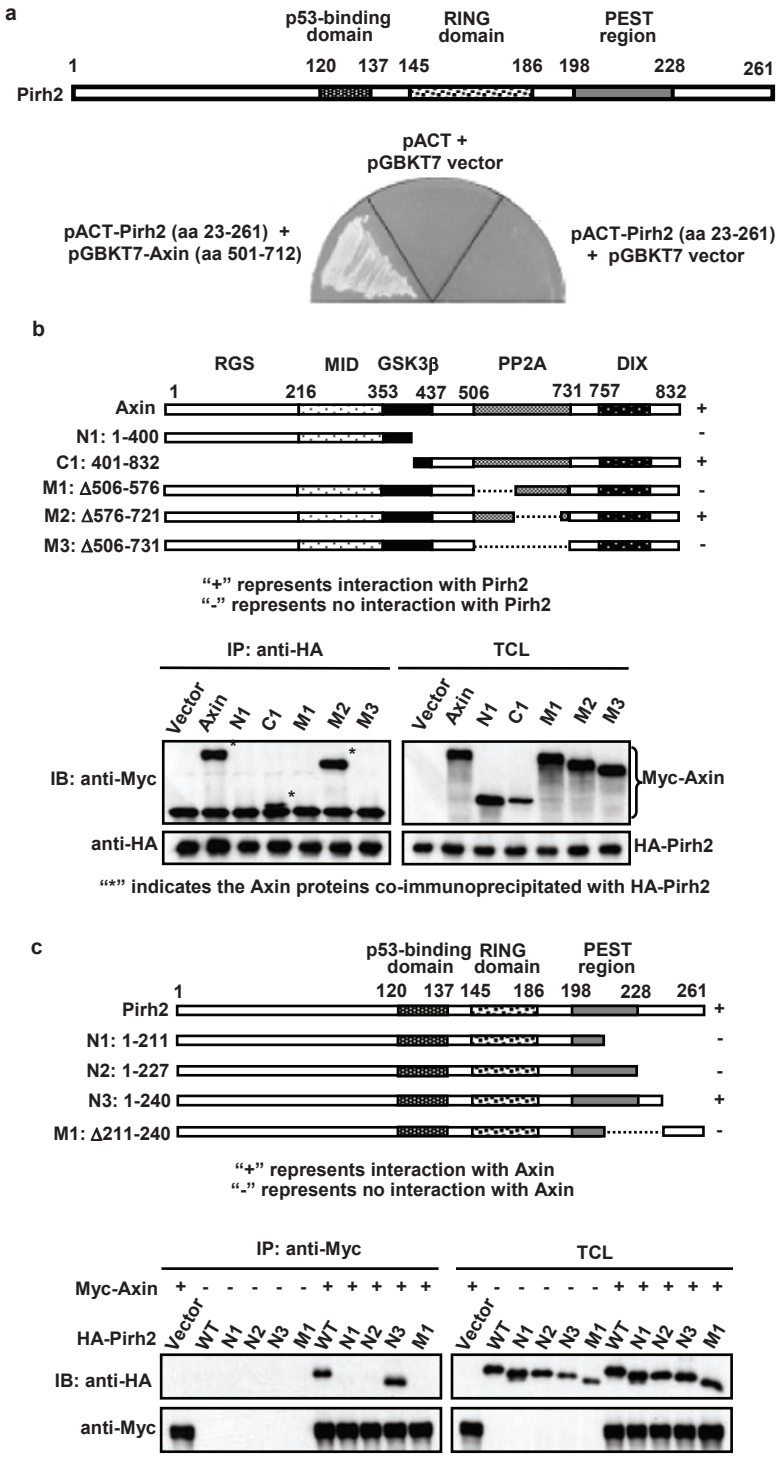

Figure S2 Pirh2 is a novel Axin-interacting protein **(a)** Yeast two-hybrid screen was performed by using the fragment of aa 501-712 of mouse Axin as bait, and one of the clones identified in the pACT fish vector, as previously described[1] encodes aa 23-261 of Pirh2. **(b)** Identification of the interacting domain of Axin for Pirh2. HA-tagged Pirh2 was cotransfected into HEK293T cells separately with pCMV5-Myc blank vector (lane 1), pCMV5-Myc-Axin (lane 2) and a series of Myc-tagged Axin mutants (lanes 3 to 7, N1, C1, M1, M2 and M3 as depicted in the schematic diagrams on the top). Cell lysates were immunoprecipitated with anti-HA antibody. Immunoprecipitates and TCL (total cell lysates) were analyzed by western blotting with anti-HA for Pirh2 and anti-Myc for Axin. The results indicate that the region of aa 506-576 of Axin interacts with Pirh2. **(c)** Identification of the Pirh2 domain for Axin interaction. Myc-tagged Axin was cotransfected into HEK293T cells with pCMV5-HA blank vector (lane 1), pCMV5-HA-Pirh2 (lane 2) and a series of HA-tagged Pirh2 deletion mutants. Cell lysates were immunoprecipitated with anti-Myc antibody. Immunoprecipitates and total cell lysates were analyzed by western blotting with anti-HA for Pirh2 and anti-Myc for Axin. This mapping result together with that in **b** shows that aa 506 of Axin interacts with aa 211-240 of Pirh2.

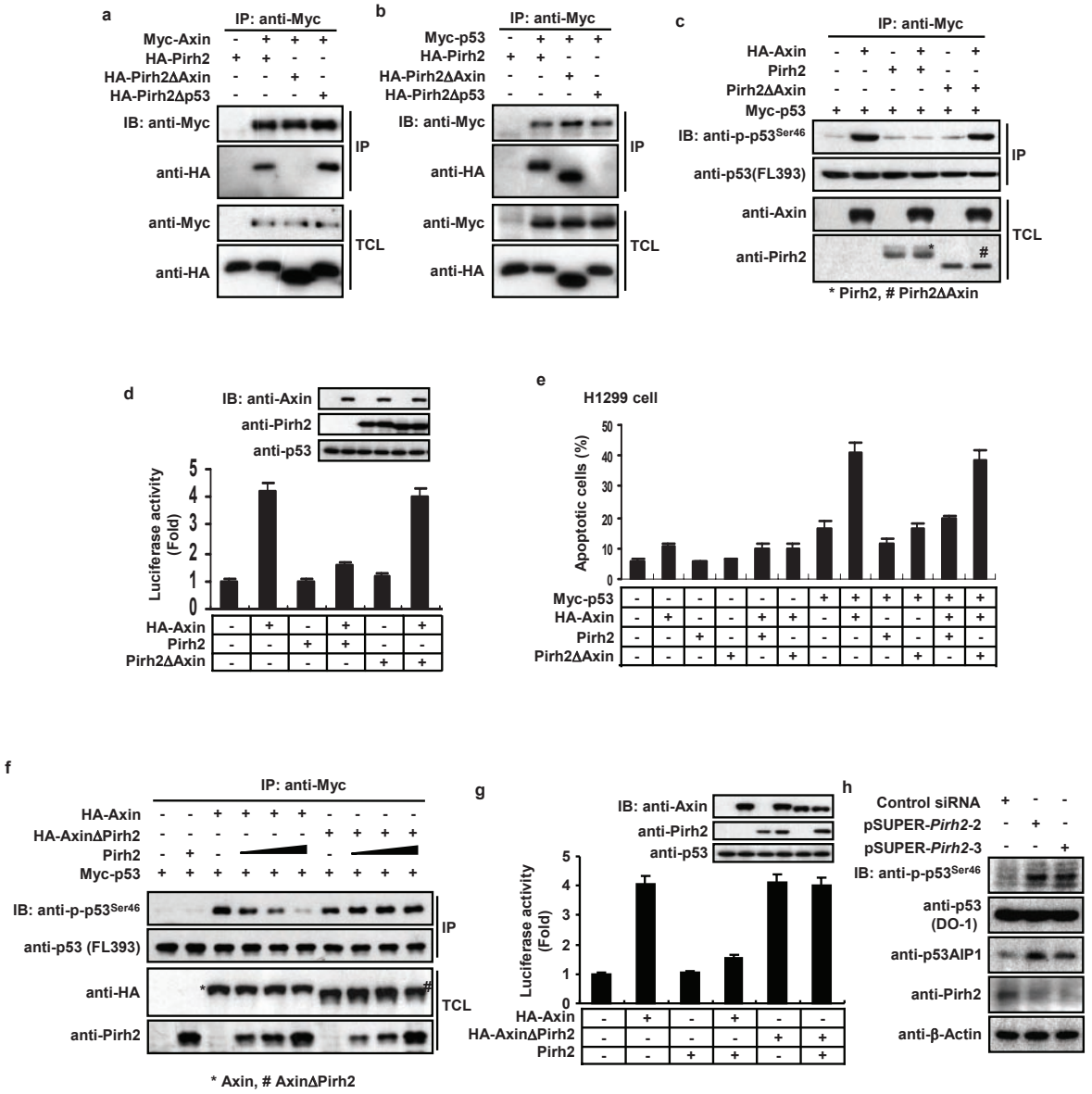

Figure S3 Pirh2 inhibits p53 activity and apoptosis induced by Axin. **(a) (b)** Pirh2Δp53 binds to Axin with an indistinguishable affinity from that of Pirh2 for Axin; Pirh2ΔAxin can bind to p53 as efficiently as wildtype Pirh2. U2OS cells were transfected with Pirh2, Pirh2ΔAxin or Pirh2Δp53 together with Axin or p53. Immunoprecipitations were carried out against Axin or p53, immunoprecipitates and total cell lysates were analyzed by western blotting with anti-HA for Pirh2 and anti-Myc for Axin or p53. **(c)** Pirh2 abrogates Axin-induced p53 phosphorylation at Ser-46. Myc-p53 was co-transfected with Axin, Pirh2 or Pirh2ΔAxin into H1299 cells. At 30 h posttransfection, Myc-p53 was immunoprecipitated followed by western blotting with anti-phospho-p53^{Ser-46} to detect levels of phosphorylated p53^{Ser-46}, and with anti-p53 (DO-1) to determine the total amount of p53 immunoprecipitated. Total cell lysates were analyzed for expression levels of Axin and Pirh2 by using anti-HA and Pirh2 polyclonal antibody, respectively. Pirh2, but not Pirh2ΔAxin, inhibits p53^{Ser-46} phosphorylation activated by Axin, indicating that physical interaction with Axin is required for Pirh2 to abolish Axin-induced p53^{Ser-46} phosphorylation. **(d)** Pirh2 inhibition of Axin-stimulated p53 transactivational activity depends on its interaction with Axin. H1299 cells were transfected with the expression plasmids of HA-Axin, Pirh2 or Pirh2ΔAxin alone or in different combinations as indicated, together with p53, p53-Luc reporter and pCMV5-LacZ. At 24 h posttransfection, luciferase activities were measured. Results are presented as means±s.e.m. of five independent experiments. **(e)** Effect of Pirh2 or Pirh2ΔAxin on Axin-induced p53-dependent apoptosis in H1299 cells. The cells were transfected with the combinations of plasmids as indicated, together with or without trace amount (10 ng) of Myc-p53. At 30 h posttransfection, apoptotic cells were counted and apoptosis rates are presented as means±s.e.m. of three independent experiments. **(f)** Pirh2 cannot inhibit AxinΔPirh2-stimulated p53 phosphorylation at Ser-46. To assess if Pirh2 could attenuate p53^{Ser46} phosphorylation stimulated by AxinΔPirh2 that is defective in binding to Pirh2, increasing amounts of Pirh2 (1, 2, 4 μg, respectively) were co-transfected with AxinΔPirh2 (2 μg), followed by IP for p53. The immunoprecipitates were probed with anti-phospho-p53^{Ser46} as described above. **(g)** Pirh2 inhibits Axin-stimulated but not AxinΔPirh2 stimulated p53 transcriptional activity. H1299 cells were transfected with expression plasmids of Axin, AxinΔPirh2 and Pirh2 in combinations as indicated, together with p53, p53-Luc reporter and pCMV5-LacZ. At 24 h posttransfection, cells were harvested and measured for luciferase activities. Results from five independent experiments are presented as means±s.e.m. **(h)** Knockdown of *Pirh2* increased p53AIP1 expression. U2OS cells were transfected with control siRNA, pSUPER-*Pirh2*-2 or pSUPER-*Pirh2*-3. 24 h posttransfection, cells were lysed and the total cell lysates were subjected to western blotting against phospho-p53^{Ser46}, p53, p53AIP1 and β-Actin with respective antibodies.

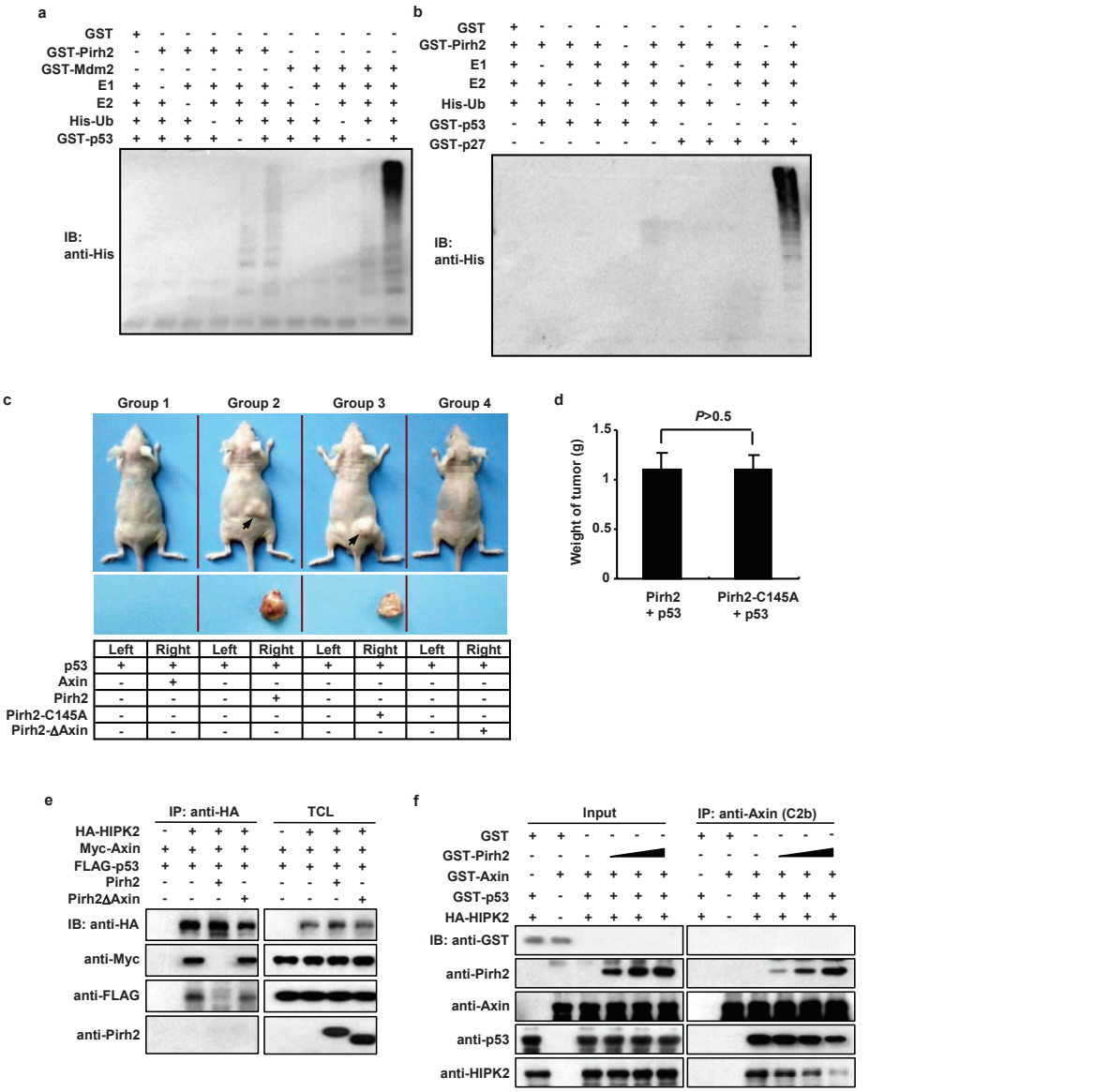

Figure S4 E3 ligase activity of Pirh2 is dispensable in its inhibition of p53 function. **(a)** Pirh2 did not exhibit any E3 ligase activity towards p53 *in vitro*. *In vitro* ubiquitination reactions containing different combinations of components were performed, using GST-p53 as substrate. The resultant samples were then subjected to western blotting using anti-His antibody to detect poly-ubiquitinated products. **(b)** Pirh2 exhibit E3 ligase activity towards p27 but not p53 *in vitro*. E1, E2, His-Ub and GST-Pirh2 together with GST-p53 or GST-p27 were incubated in ubiquitination buffer for 2 h. The reaction were stopped by adding 2 × SDS sample buffer and western blotting was performed with anti-His antibody. **(c)** Interaction with Axin, but not its E3 ligase activity, is required for Pirh2 to promote xenograft tumor growth. H1299 cells were transfected with trace amount (10ng) of p53 and 0.3 μg of pcDNA6.0 vector carrying blasticidin resistant gene, together with or without 5 μg of Axin or Pirh2-C145A or Pirh2 ΔAxin. Some 24 h after transfection, cells were selected with 10 μg/ml of blasticidin for one week. The resistant cell were then collected and $5\times10P^{6P}$ cells were used for each injection. The left side of all of the nude mice was injected with cells expressing p53 alone as control; the right side of each mouse was injected with cells co-expressing p53 and Axin (Group 1), Pirh2 (Group 2), Pirh2-C145A (Group 3), or Pirh2-ΔAxin (Group 4). Each combination of injections was performed in triplicate. Six weeks later, tumors were removed for photo-taking, and determination of weight for statistical analysis. Representative whole mice are shown. It is evident that cells expressing p53 alone did not develop into tumor (left side of each mouse), whereas the cells co-expressing p53 and wildtype Pirh2 or Pirh2-C145A mutant grew into tumors of similar sizes. Of important note, Pirh2-ΔAxin did not promote tumor growth. **(d)** Statistical analysis (Student's *t*-test) of the tumor weights for comparison between p53/Pirh2-expressing cells and p53/Pirh2-C145A-expressing cells. The values are represented as mean±s.e.m. of three independent experiments in triplicates. **(e)** Pirh2ΔAxin does not compete against HIPK2 for binding with the Axin-p53 complex. Myc-Axin and FLAG-p53 were cotransfected into H1299 cells with HA-HIPK2, Pirh2 and Pirh2ΔAxin in different combinations as indicated. Anti-HA antibody was used to immunoprecipitate HA-HIPK2 and western blotting was carried out to detect Axin, HIPK2, p53 and Pirh2 in the immunoprecipitates. Axin-p53 complex was excluded from interacting with HIPK2 in the presence of Pirh2, but not in the presence of Pirh2ΔAxin. **(f)** Pirh2 competes against HIPK2 binding to Axin-p53 complex *in vitro*. HA-HIPK2 was transfected into H1299 cells and immunoprecipitated with anti-HA antibody, and then dissociated from beads by elution with HA peptide. The HA-HIPK2 was then mixed in lysis buffer containing GST, GST-Pirh2, GST-Axin and GST-p53 in combination as indicated. After 3 h of incubation, GST-Axin was immunoprecipitated with anti-Axin antibody (C2b). The inputs and the immunoprecipitates were then subjected to western blotting with anti-GST, anti-Pirh2, anti-p53, anti-Axin and anti-HIPK2 antibodies as indicated.

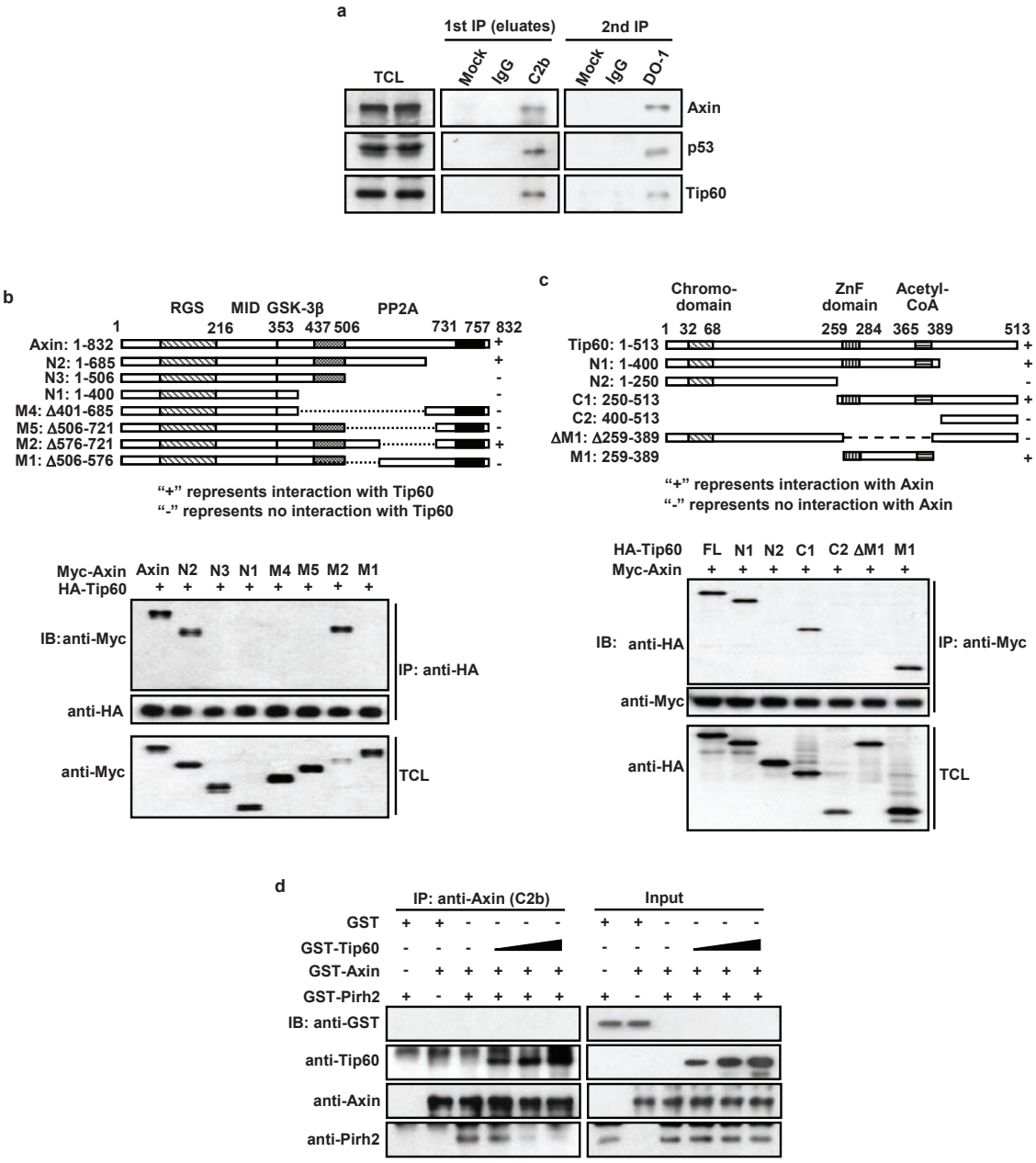

Figure S5 Tip60 is a novel Axin-interacting protein. **(a)** Axin, Tip60 and p53 form a ternary complex assessed by two-step co-IP using U2OS cell lysates. **(b)** Identification of the Axin domain responsible for interacting with Tip60. HEK293T cells were transfected with HA-Tip60 and a series of Myc-tagged Axin deletion mutants as depicted in the diagrams. HA-Tip60 was immunoprecipitated, and the precipitates and TCLs were then subjected to western blotting with anti-Myc and anti-HA antibodies. **(c)** Identification of the Tip60 domain responsible for interacting with Axin. Myc-tagged Axin was cotransfected into HEK293T cells with pCMV5-HA-Tip60 or a series of HA-tagged Tip60 mutants (lanes 2 to 7, depicted in schematic diagrams on the top). Cell lysates were immunoprecipitated with anti-Myc antibody. Immunoprecipitates and total cell lysates were analyzed by western blotting with anti-HA for Tip60 and anti-Myc for Axin. **(d)** Recapitulation of the competitive binding between Tip60 and Pirh2 to Axin *in vitro*. Reconstitution of purified GST-Axin, GST-Pirh2 with increasing amounts of Tip60 was performed. After 3 h of incubation, Axin was immunoprecipitated with anti-Axin antibody (C2b). The inputs and the immunoprecipitates were then subjected to western blotting with anti GST, anti-Tip60, anti-Axin and anti-Pirh2 antibodies as indicated. The result shows that Tip60 is able to compete against Pirh2 binding to Axin.

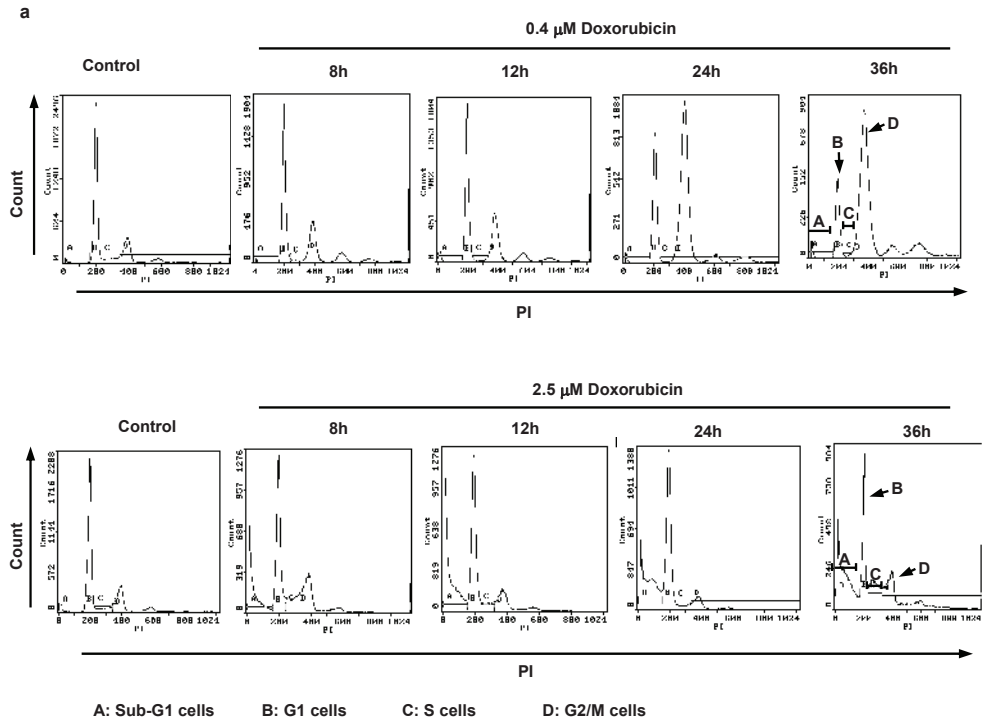

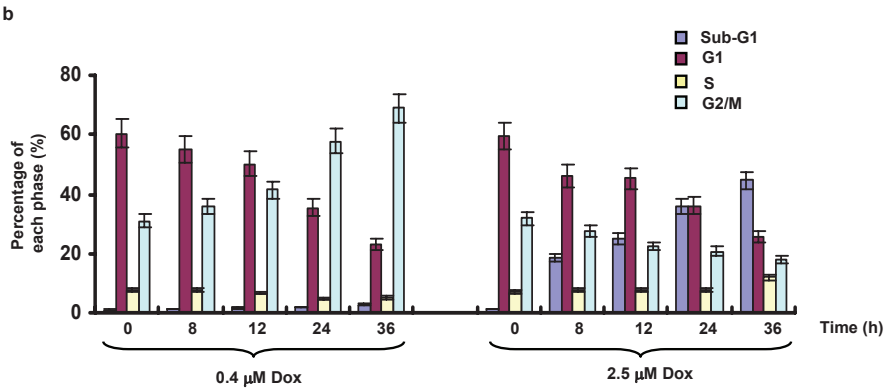

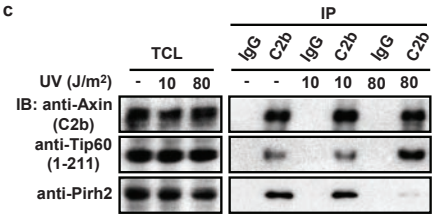

Figure S6 Determination of sublethal and lethal doses of Dox for U2OS cells. **(a)** Cells were treated with different doses of Dox (0.1 μM to 5.0 μM), and after 8, 12, 24, or 36 h of incubation the cells were subjected to flow cytometry analysis. Shown here are representative graphs of cell cycle distribution of U2OS cells treated with 0.4 μM Dox and 2.5 μM Dox, respectively. **(b)** Statistical analysis of Dox treated cells in **a** for their cell cycle distribution. It was found that cells undergo cell cycle arrest under 0.4 μM Dox treatment with cells enriched at G2/M phase, and apoptosis under 2.5 μM Dox treatment with sub-G1 cells increased. The values are shown as mean±s.e.m. of three independent experiments. **(c)** Decreased levels of Pirh2 and increased levels of Tip60 are associated within Axin under lethal dose UV treatment. U2OS cells were exposed to 10 J/m^2 or 80 J/m^2 UV and kept in culture medium for 8 h. IP was then performed with anti-Axin antibody (C2b) to pull down Axin complexes in the cell lysates. Cell lysates and immunoprecipitates were then subjected to western blotting with anti-Axin, anti-Tip60 (1-211) and anti-Pirh2 antibodies as indicated.

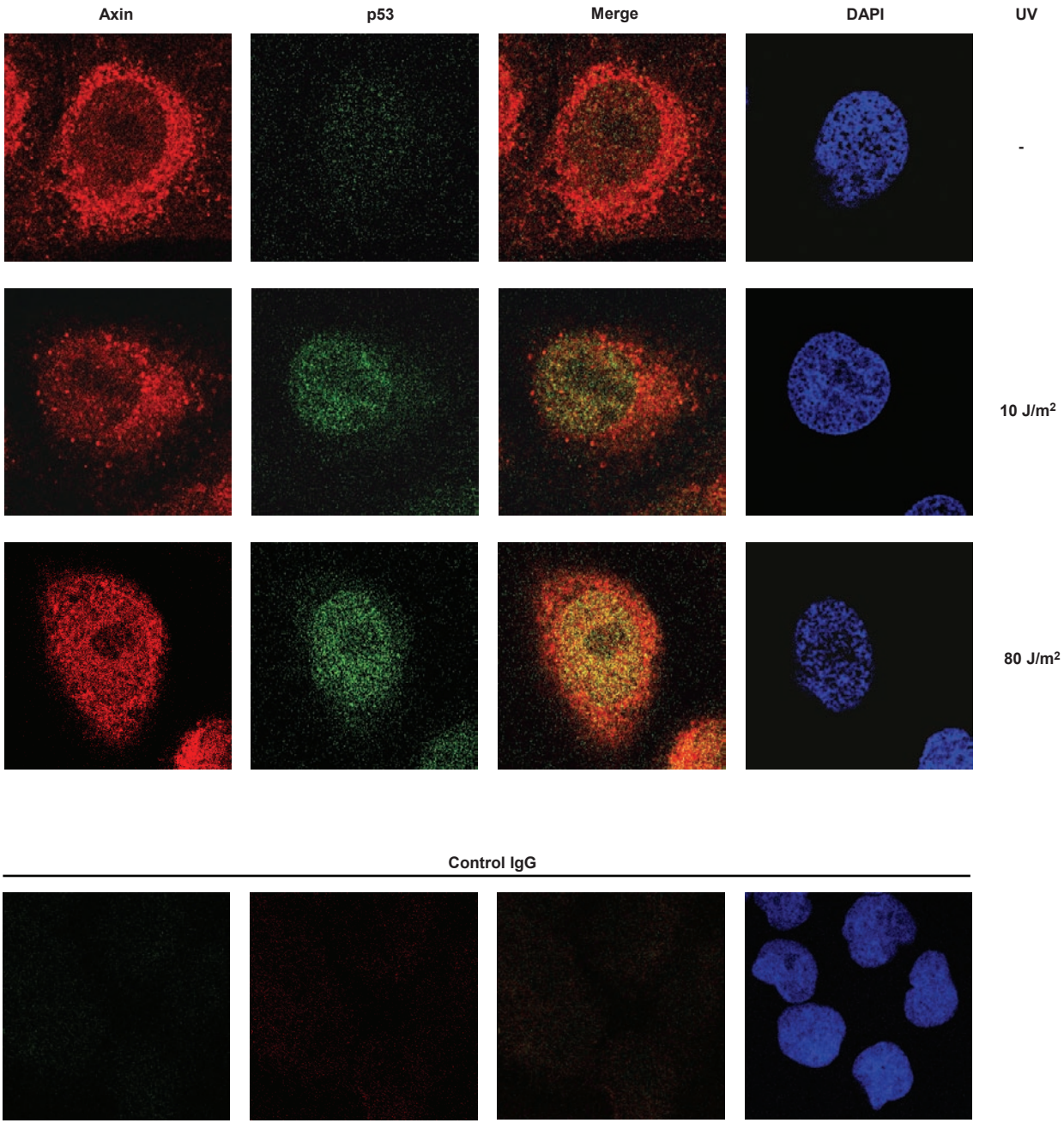

Figure S7 Immunofluorescent staining of endogenous Axin and p53. U2OS cells were untreated or treated with 10 J/m2 or 80 J/m2 UV, and were subjected to immunostaining at 4 h post-treatment as described in Supplementary Methods. Mock IgG was used as control. Upon UV treatment, p53 levels and nuclearly localized Axin were increased; enhanced co-localization of Axin and p53 was seen in lethally treated cells.

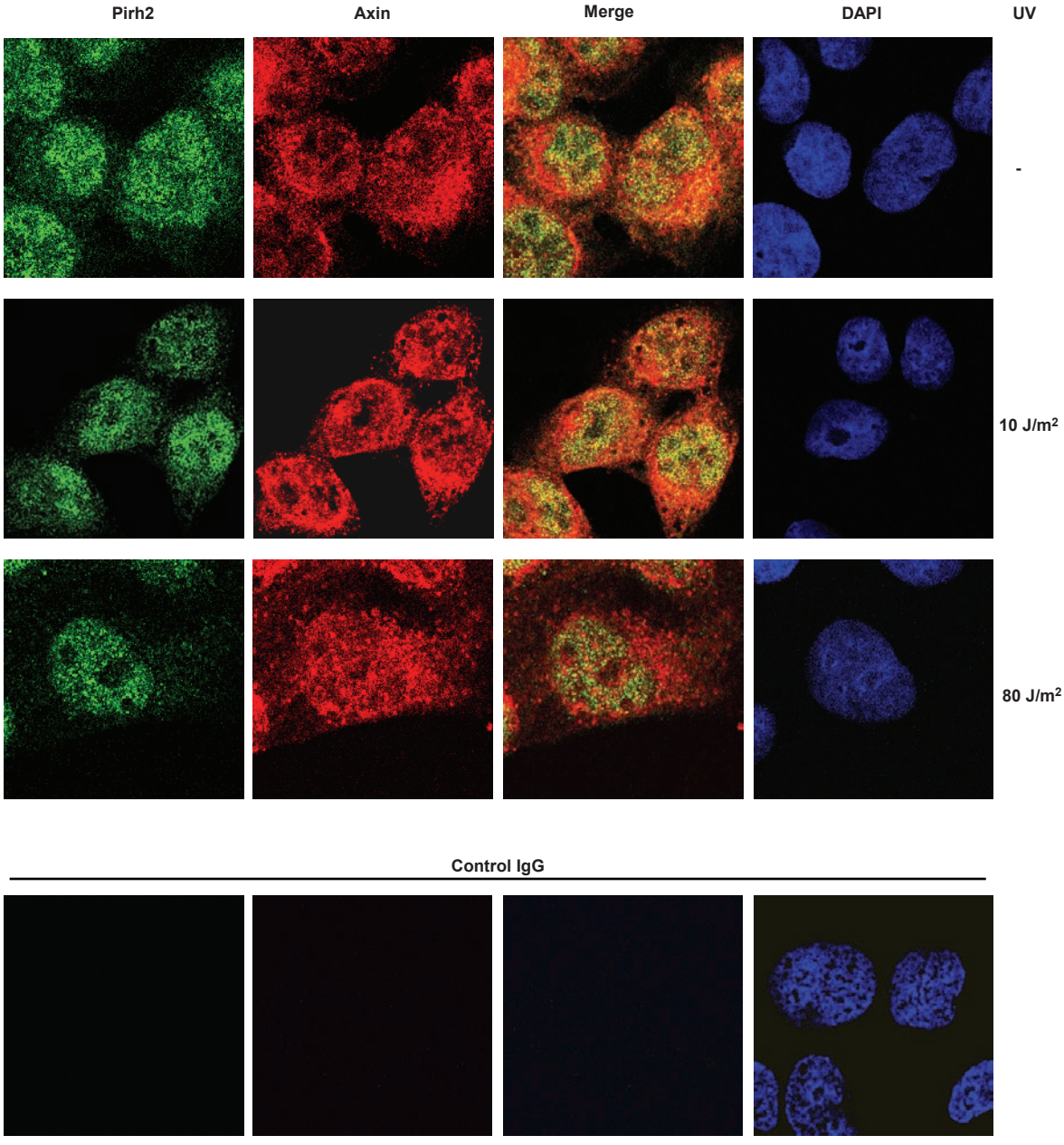

Figure S8 Immunofluorescent staining of endogenous Axin and Pirh2. Experimental procedures are as described above. In untreated and sublethally treated cells, colocalization between Axin and Pirh2 was detected in both the nucleus and the cytoplasm. In lethally treated cells, Axin interaction with Pirh2 was diminished.

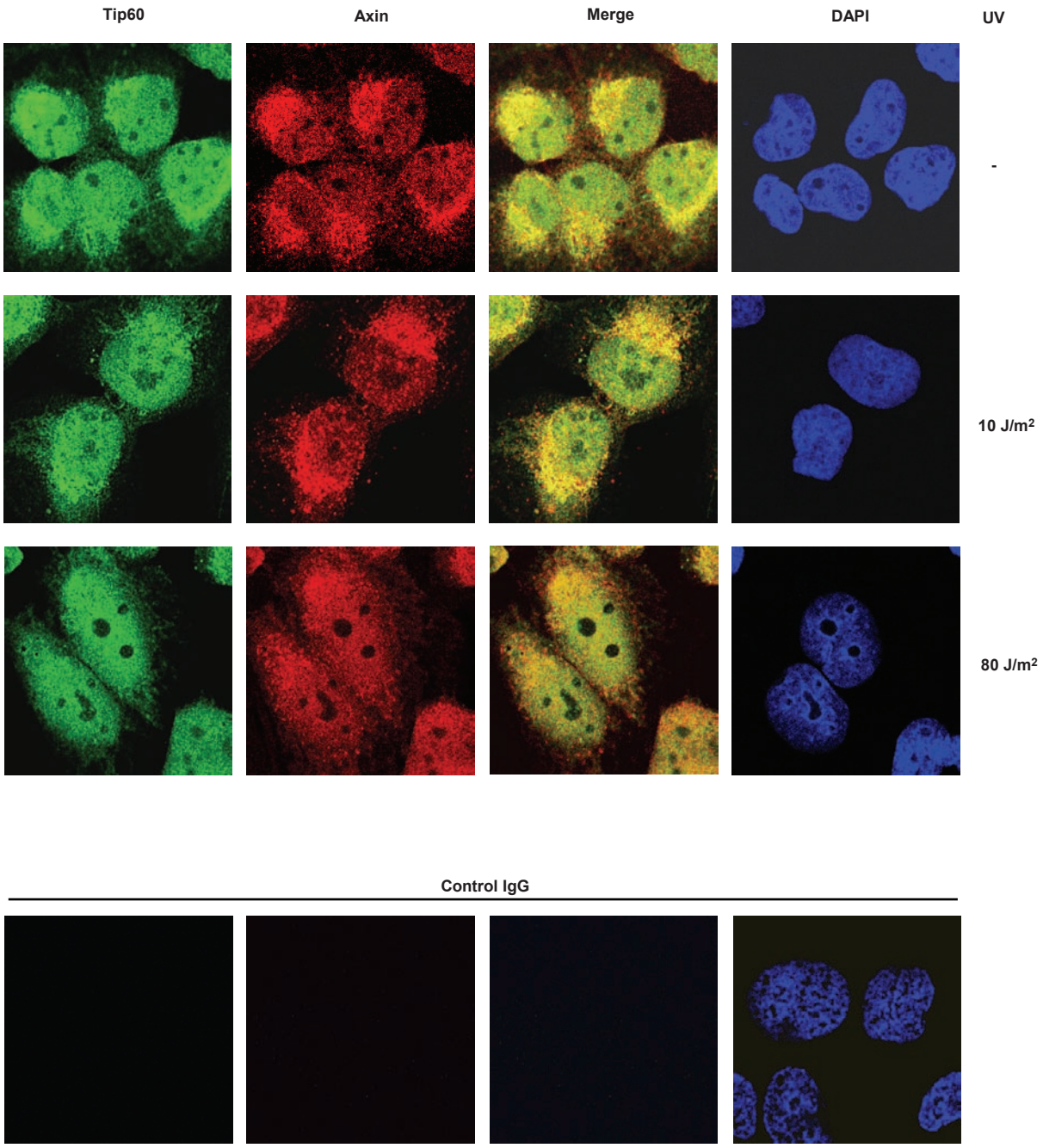

Figure S9 Staining of endogenous Axin and Tip60 in U2OS cells. Note that in untreated and sublethally treated cells, Axin is colocalized with Tip60 mostly in the perinuclear areas; in lethally treated cells, their increased colocalization is observed in the nucleus.

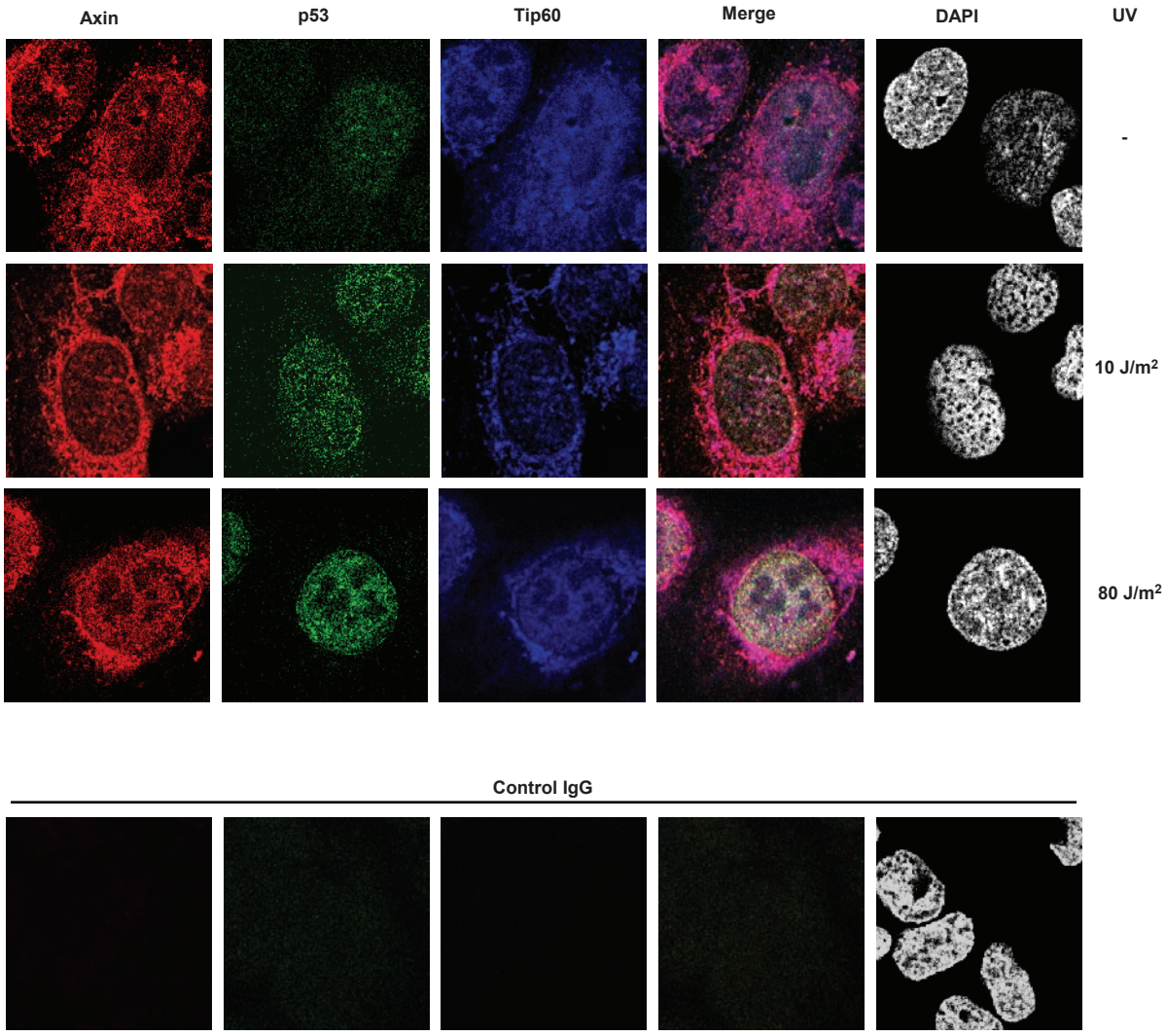

Figure S10 Triple costaining of endogenous Axin, p53 and Tip60 in U2OS cells. Note that in lethally treated cells, prominent colocalization signal (white color after merging) is detected in the nucleus.

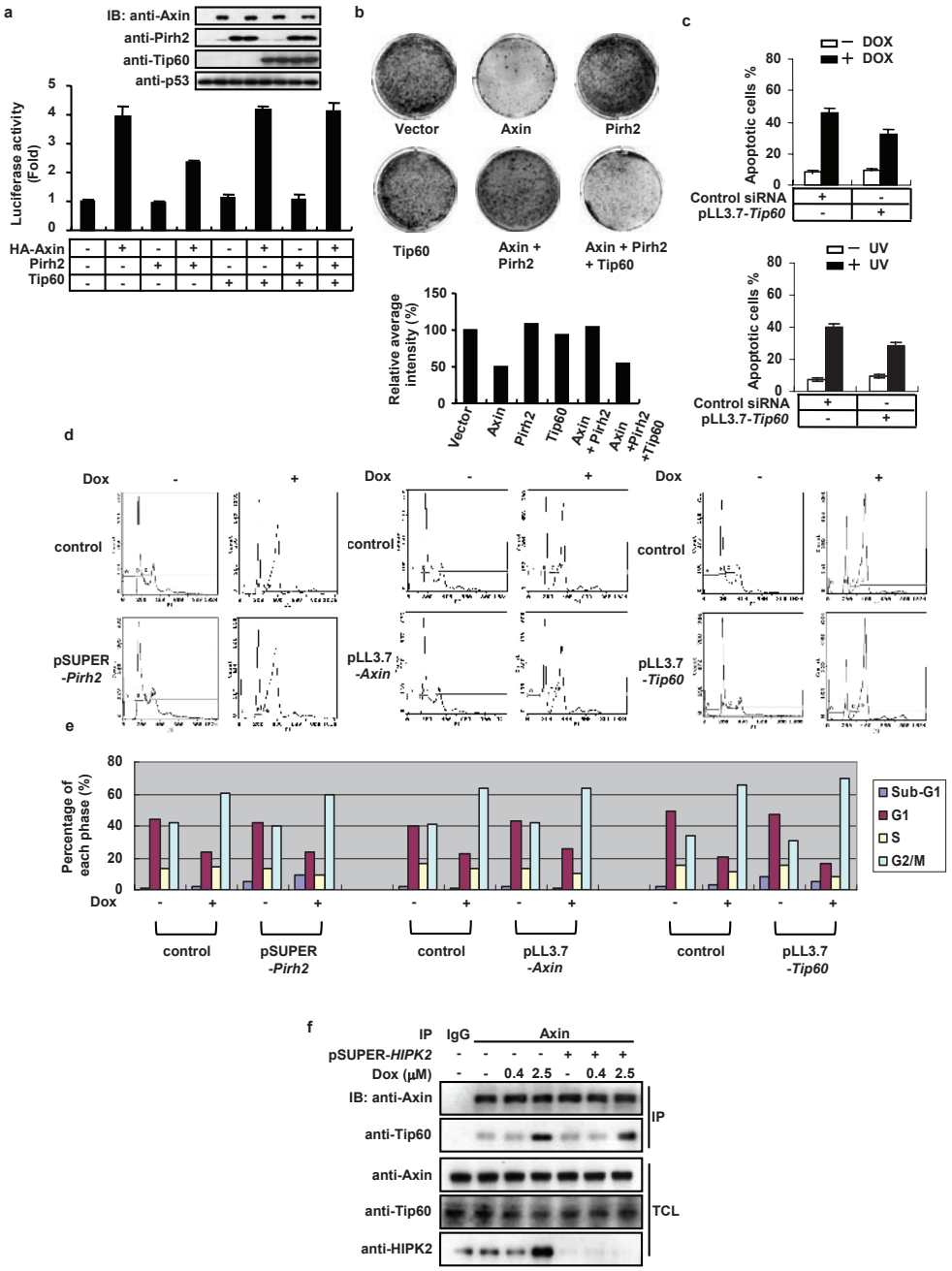

Figure S11 (a) Tip60 overcomes the inhibitory effect of Pirh2 on Axin-stimulated p53 transactivational activity. H1299 cells were transfected with Axin, Pirh2 and Tip60 in different combinations as indicated, together with trace amount of p53, p53-Luc and LacZ. Luciferase activities were measured after 24 h of transfection and the values were normalized to LacZ activities. Results of three independent experiments are presented as means±s.e.m. **(b)** Tip60 reverses the inhibition of Pirh2 on Axin-induced cell death of U2OS cells determined by colony formation assay. U2OS cells were transfected with Axin, Pirh2 and Tip60 alone or in combination as indicated, together with 0.1 μg of pcDNA6.0. At 24 h posttransfection, blasticidin was added into medium to select for transfected cells. Cells were cultured for another 10 days and then stained with crystal violet. The average intensity of each plate was calculated by Totallab TL100 software. **(c)** Knockdown of *Tip60* reduces apoptosis rates induced by lethal DNA damage. U2OS cells were infected with lentiviral pLL3.7 harboring control siRNA or siRNA against *Tip60*. Cells were treated with 2.5 μM Dox (left) or 80 J/m^2 UV (right). 24 h later, apoptotic cells were counted after Hoechst staining. Error bars, s.e.m.; n=3. **(d)** Depletion of Axin, Pirh2 or Tip60 has no significant effect on cell cycle progression or cell cycle arrest caused by sublethal DNA damage. U2OS cells were transfected with pSUPER-*Pirh2* or control siRNA together with 0.3 μg of pcDNA6.0 vector carrying blasticidin resistant gene. Some 24 h after transfection, cells were selected with 10 μg/ml of blasticidin for one week. Axin- and Tip60-depleted cells were generated by lentivirus mediated siRNA using pLL3.7-*Axin* and pLL3.7-*Tip60*. After 24 h of incubation with 0.4 μM Dox, the cells were subjected to flow cytometry analysis. **(e)** Percentage of cells in each cell-cycle phase as assayed in **d**. **(f)** Knockdown of *HIPK2* has no effect on Tip60-Axin interaction in cells lethally treated with Dox. U2OS cells were transfected with control siRNA or pSUPER-*HIPK2*. At 20 h posttransfection, cells were left untreated or treated with 0.4 μM or 2.5 μM Dox for 18 h. The cell lysates were immunoprecipitated by anti-Axin (C2b). The immunoprecipitates and total cell lysates were analyzed with antibodies indicated.